Since January 2020 Elsevier has created a COVID-19 resource centre with free information in English and Mandarin on the novel coronavirus COVID-19. The COVID-19 resource centre is hosted on Elsevier Connect, the company's public news and information website.

Trends in Analytical Chemistry 161 (2023) 116999

Contents lists available at ScienceDirect

Trends in Analytical Chemistry

journal homepage: www.elsevier.com/locate/trac

Fluorescent detection of emerging virus based on nanoparticles: From synthesis to application

Qian Xu, Fangbin Xiao, Hengyi Xu*

State Key Laboratory of Food Science and Technology, Nanchang University, Nanchang, 330047, PR China

ARTICLE INFO

Article history:
Received 3 November 2022
Received in revised form
26 January 2023
Accepted 21 February 2023
Available online 23 February 2023

Keywords:
Emerging virus
Fluorescence nanoparticles
Fluorometric sensors
Detection
Public health

ABSTRACT

The spread of COVID-19 has caused huge economic losses and irreversible social impact. Therefore, to successfully prevent the spread of the virus and solve public health problems, it is urgent to develop detection methods with high sensitivity and accuracy. However, existing detection methods are time-consuming, rely on instruments, and require skilled operators, making rapid detection challenging to implement. Biosensors based on fluorescent nanoparticles have attracted interest in the field of detection because of their advantages, such as high sensitivity, low detection limit, and simple result readout. In this review, we systematically describe the synthesis, intrinsic advantages, and applications of organic dye-doped fluorescent nanoparticles, metal nanoclusters, up-conversion particles, quantum dots, carbon dots, and others for virus detection. Furthermore, future research initiatives are highlighted, including green production of fluorescent nanoparticles with high quantum yield, speedy signal reading by integrating with intelligent information, and error reduction by coupling with numerous fluorescent nanoparticles.

1. Introduction

Viruses are infectious pathogens that can cause significant infectious diseases by destroying cells, tissues, and organs [1]. A wide range of human diseases are brought on by viruses, including common illnesses like influenza and chickenpox identified, as well as devastating diseases such as smallpox, Acquired Immune Deficiency Syndrome (AIDS), Severe Acute Respiratory Syndrome Coronavirus 2 (SARS-CoV-2), Ebola hemorrhagic fever, and avian influenza [2–5]. The SARS-CoV-2, which has killed more than 6 million individuals since its discovery in late 2019 (as of 6:58 p.m. CEST, 7 September 2022), is currently spreading and changing throughout the world, and the number of new cases is continuously rising quickly (Fig. 1). Numerous viruses have killed billions of people, caused tremendous economic losses, and had a permanent negative impact on society. Viruses are not immutable and may mutate [6], which may reduce the effectiveness of a vaccine, making a challenging and complex process of a successful drug or vaccine [7,8]. On the other hand, timely detection and prevention of the virus are efficient ways to successfully block it [9]. Therefore, it is critical to develop rapid and effective virus detection technologies [10].

Traditional virus detection methods include virus culture, reverse transcription-polymerase chain reaction (RT-PCR), and enzyme-linked immunosorbent assay (ELISA) [11,12]. When it comes to nucleic acid amplification using a fluorescent reporter for the diagnosis of new coronaviruses, RT-PCR has been regarded as the gold standard. RT-PCR experiments are typically separated into three steps: the first step is the extraction of viral RNA, the second step is a reverse transcription into complementary DNA (cDNA), and the third step is the amplification of cDNA for detection using the polymerase chain reaction (PCR). The RT-PCR technique is highly sensitive and accurate, but it requires expensive specialized equipment and complex sequence comparison primer construction, which takes time and should be performed in a well-trained laboratory [13]. ELISA is a rapid assay for identifying viral antigens, but its low sensitivity and the requirement for high-quality sample preparation limit its application in point-of-care testing [14]. Furthermore, virus culture is a time-consuming job that necessitates the use of trained individuals and precise methodologies, these have restricted its use in the field of rapid virus detection.

To overcome the problems associated with conventional diagnostic techniques, alternative reliable virus detection with high sensitivity and accuracy should be developed. Among the various

* Corresponding author. State Key Laboratory of Food Science and Technology, Nanchang University, 235 Nanjing East Road, Nanchang, 330047, PR China.
E-mail addresses: kidyxu@163.com, HengyiXu@ncu.edu.cn (H. Xu).

https://doi.org/10.1016/j.trac.2023.116999
0165-9936/

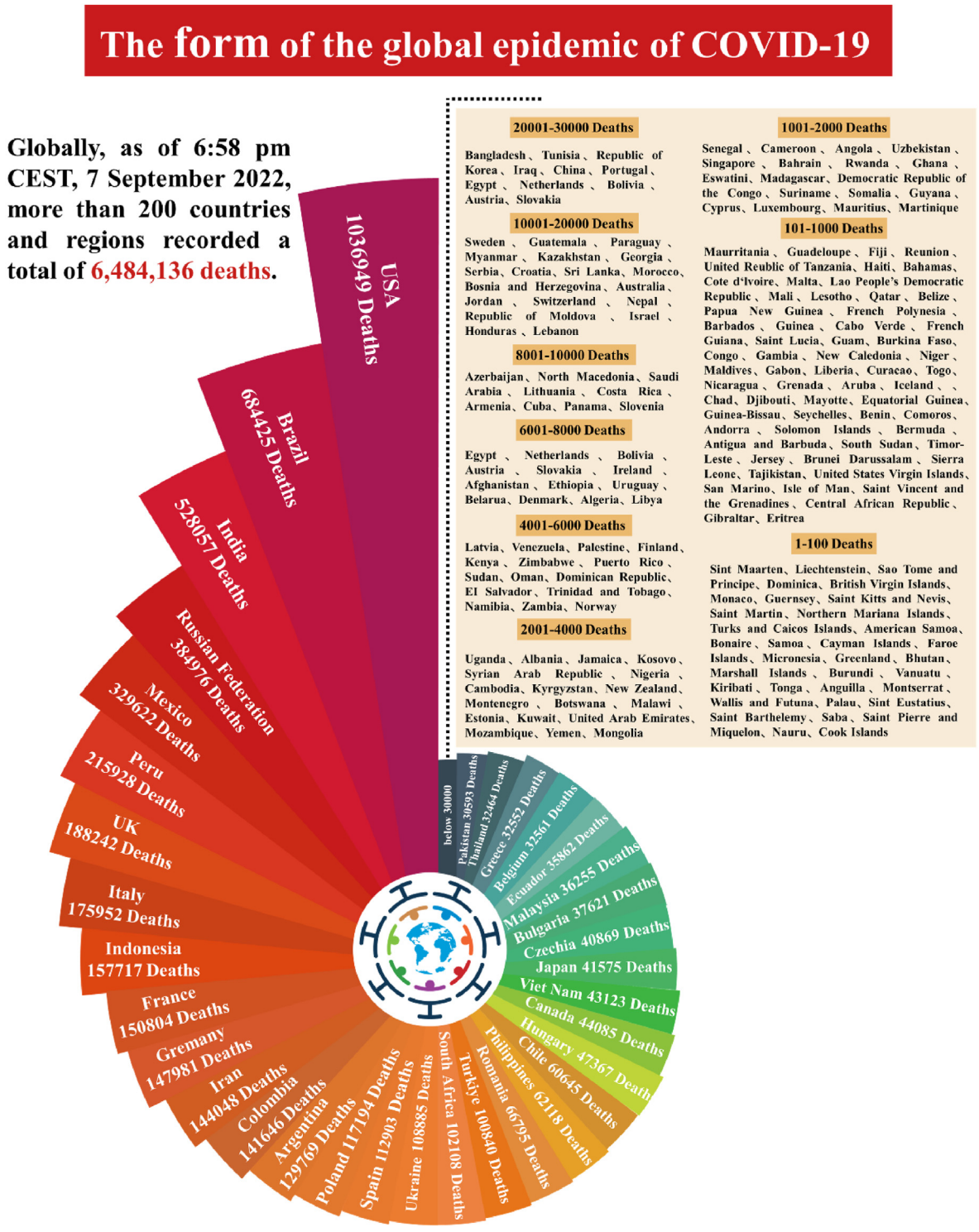

Fig. 1. COVID-19 deaths by region and country. The data source: World Health Organization (WHO).

methods of detecting viruses, fluorescent assays are popular [15]. Due to their great sensitivity, simplicity of use, and real-time, emerging fluorescence techniques are extensively used in medical diagnostics and other sectors [16]. Considering their unique physicochemical characteristics, numerous nanomaterials have made significant developments and breakthroughs in bioanalysis [17]. Nanostructure-based biosensors benefit from flexible sensing mechanisms, high specificity and sensitivity, label-free and quick real-time detection, and other features that have sparked widespread interest in nanotechnology and biosensor research [18]. Studies integrating fluorescent biosensing devices with nanotechnology have increased in recent years. The benefits of fluorescence biosensors that enable early diagnosis and better healthcare outcomes are listed below due to their intrinsic properties: (1) High sensitivity and low detection limit. (2) Naked eye readout can be created for quick diagnosis and simple readout. (3) Low detection

cost.

However, the majority of fluorescent biosensors are associated with organic dyes [19], metal nanoclusters [20], up-conversion particles [21], and quantum dots [22], many of which may have flaws in their development such as being expensive, toxic, challenging to synthesize, or having high background interference. Therefore, it would be essential to create inexpensive fluorescent reporters with minimal toxicity that may be employed for the quick detection of viruses. Given the tremendous potential of fluorescent nanoparticles in virus detection, some relevant virus detection reviews have previously been published. However, they are either outdated or insufficiently comprehensive [18,23], and there is a strong demand for a comprehensive and systematic review paper covering various types of fluorescent nanoparticles and their applications in virus detection. In this paper, we review literature of the last decade and briefly introduce various types of fluorescent nanoparticles, primarily organic dye-doped fluorescent nanoparticles, metal nanoclusters, up-conversion particles, quantum dots, and carbon dots, with a focus on the synthesis, intrinsic advantages, and applications of fluorescent nanomaterials for virus detection (Fig. 2). Finally, present obstacles and potential future study areas are explored. Table 1 and Table 2 summarize the advantages and disadvantages of various fluorescent nanoparticles and common virus detection methods, respectively. Table 3 summarizes the application of fluorescent nanoparticles in the detection of the emerging virus.

2. Organic dye-doped fluorescent nanoparticles

Organic fluorescent dyes, which frequently formed of benzene or heterocyclic rings with conjugated double bonds. Cyanine dyes [24], rylenecarboximide (RI) dyes [25], boron dipyrromethene (BODIPY) [26], coumarins [27], and other fluorophores are now the most common. These materials are favored by individual fields due to their tiny size, a wide range of colors, and biocompatibility [28]. However, conventional fluorescent dyes often have low luminescence intensity and poor photostability under aqueous conditions, which limits their development for biomedical applications including high-quality fluorescence imaging, in vitro diagnostics, and biotherapeutics [29]. A more reliable and sensitive output of fluorescent signals may be made possible by the encapsulation of organic dyes into nanoparticles. Owing to their distinctive features, organic dye-doped fluorescent nanoparticles (ODFNs) have shown significant potential for applications. In virus detection, their employment as fluorescence-enhanced signal reporters has been extensively employed. Therefore, in this section, we will focus on the synthesis methods of organic dyes and dye-based nanoparticles and their application in virus detection.

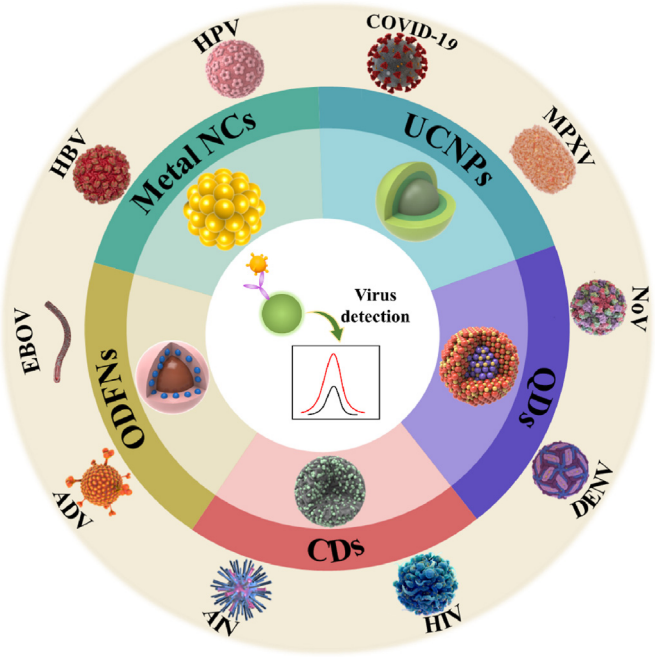

Fig. 2. Schematic illustration for fluorescent detection of emerging virus based on nanoparticles.

2.1. Synthesis and modification

In recent years, organic dyes have been chemically modified to increase their water solubility, stability, optical characteristics, and so on. The primary preparation techniques include chromophore modification, nanoscale self-assembly, supramolecular assembly, etc [30]. On the one hand, probe molecules with high fluorescence quantum yield (QY), photodynamic and photothermal capabilities can be prepared by modifying the framework of organic dyes [31]. On the other hand, functionalized alteration of the periphery of organic dyes can confer water solubility, biocompatibility, and targeting characteristics [32].

There are three primary methods for obtaining high-performance ODFNs (Fig. 3). Firstly, the chromophore skeleton is one of the keys to the application of organic dyes. Through chemical modification of organic dyes, the energy conversion pathway of dyes can be controlled, which is expected to be suitable for application scenarios. After the chromophore absorbs light, energy is released in a variety of ways, including fluorescence, thermal energy, and chemical energy. For example, by inserting the donor-acceptor (D-A) structure or expanding the conjugate, the dye's absorption wavelength can be red-shifted [33]. Chen et al. designed organic dyes with significant red-shift absorption and emission spectra through the construction of D-A structures and conjugate extension [34]. Secondly, because of their massive, conjugated structures, organic dyes have poor hydrophilicity. There are two primary strategies for increasing water solubility. One is modification employing hydrophilic functional groups (such as carboxyl, amino or amphibian groups) or hydrophilic polymers (such as dendrites, hyperbranched arms, PEG chains, and polyamine acids) [35–38]. Based on this, poly(2-aminoethyl methacrylate) and poly(2-(dimethylamino)ethyl methacrylate) are used as external polymer arms to improve the water solubility of perylene diimide through electrostatic interaction [36]. The another involves creating a topological “core-shell” macromolecular structure with hydrophilic molecules acting as the shell and organic dyes acting as the core. This technique not only safeguards the organic dyes' cores but also successfully prevents the core from aggregating and interference of the outside environment, enhancing the optical characteristics and stability [39]. Among them, sol–gel derived silica was reported as an excellent host material for creating fluorescent NPs with the covalently attached organic chromophores. For example, Qiu et al. used an unimolecular fluorescent hyperbranched conjugated polymer (HCP-star-PDMAEMA) as soft template and isolated them with a silica shell to fabricate highly fluorescent core-shell hybrid NPs HCP@SiO_2 [40]. Finally, because of their unique size and surface effects, nanomaterials have become a study hotspot. Encapsulating the dye in a polymer carrier is one method of producing nanoparticles. Controlling assembly can also be used to tune the characteristics of nanoparticles [41]. Similarly,

Table 1
Summary and comparison of advantages and disadvantages of various fluorescent nanoparticles.

Fluorescent nanoparticle	Advantages	Disadvantages	Synthetic methods	Reference
ODFNs	Low cost Simple and straightforward acquisition Various categories Easy surface modification High fluorescence quantum yield	Fluorescence dye quenching Low sensitivity Poor stability High native background	Chromophore modification	[31,33]
			Supramolecular assembly	[32,34–38]
			Nanoscale self-assembly	[41,43]
MNCs	Simple and easy to synthesis Large Stokes shift Good biocompatible Remarkable photophysical properties	Low quantum yield Difficult to surface modification Poor stability	Monolayer-protected method	[91]
			Template method	[75,80,82,84–87]
			Chemical etching method	[93]
			Microwave-assisted method	[72]
UCNPs	Excellent up-conversion ability Strong signal penetration Adjustable optical No background fluorescence interference Good photostability Easy to surface modification	Expensive instrument Poor chemical stability Low luminescence efficiency Difficult to synthesis	Thermal decomposition method	[118–121]
			Coprecipitation method	[122–126]
			Hydrothermal method	[128–131]
QDs	High fluorescence quantum yield Broad excitation peak tunable emission Superior photostability Diverse surface modification	Poor chemical stability Low sensitivity Strong intrinsic toxicity Great environmental harm Background interference	Organic phase synthesis	[150–154]
			Aqueous phase synthesis	[155–159]
CDs	Wide range of raw materials Excellent biocompatibility High specific surface area Outstanding photostability Low toxicity Good water solubility High quantum yield	Small particle size leads to fluorescence quenching easily Difficult to synthesize the CDs with long wavelengths	Top-down method	[186,187,192,195]
			Bottom-up method	[204,207,209]

Table 2
Summary and comparison of common virus detection methods.

Detection method	Detection time	Advantage	Disadvantage	Reference
Virus culture	Days to weeks	Broad spectrum Inexpensive High accuracy	Time-consuming Complex steps Contamination problems	[49]
RT-PCR	Hours	High sensitivity Accurate detection result	Expensive equipment Highly skilled analysts Time-consuming Extremely liable to contamination	[19]
ELISA	Hours	Only one incubation step No hook effect at high analyte concentrations	Poor sensitivity Depend on specialized equipment	[59]
ECL	Hours	Simple device requirement Low background noise High sensitivity Wide dynamic range	Sensitive to sample matrix effect Small temperature range Short service life	[96]
High-throughput multiplex coding	Minutes	Simultaneous detection Save reagents and specimens	Poor sensitivity High material requirements	[145]
MRSw	Minutes	Simplify the assay steps Achieve closed-loop detection Enable near background-free sensing High signal-to-noise ratio	Non-specific aggregation of MNPs Unsatisfactory sensitivity	[181]
LFA	Minutes	User-friendly operation Rapid delivery of results Low cost Easy scalability to high-volume production	Low sensitivity High false negative rates	[168]

Sauer et al. combined surface activity, polymerizability, and fluorescent property into a single molecule to create a luminous surfmer (surfactant monomer). Fluorescent surface-labeled polystyrene (PS) NPs were produced using miniemulsion polymerization employing the fluorescent surfmer. By employing certain polymerization, this method could have the ability to produce fluorescent NPs with controllable size. Additionally, while designing a material and analyzing its characteristics, the steric hindrance of polymeric nanoparticles should be considered [42]. Additionally, drug-loaded micelles, host-guest complexes, and metal-organic frameworks (MOFs) structures can be formed through the supramolecular assembly of organic dyes with other molecules, indicating considerable potential in drug delivery, virus diagnostics, and virus imaging, among other applications [43].

2.2. Application of virus detection

When organic fluorescent dyes are brought back to their ground state from their excited state, energy is released in the form of light emission. Organic fluorescent dyes may be employed as fluorescent signal reporters in a variety of sectors thanks to their emission intensity, color, and responsiveness, which can be achieved by careful structural design. Encapsulating a single fluorophore in a nanomaterial and combining two or more fluorophores with various emission colors are the two basic methods used to create an organic dye-based fluorescent signal reporter [44]. This section will concentrate on recent breakthroughs in conventional organic dye-doped fluorescent nanoparticles, aggregation-induced emission luminophore (AIEgens)-doped fluorescent nanoparticles (AIEFNs),

Table 3
Summary of the application of fluorescent nanoparticles in the detection of the emerging virus.

Analyte	Fluorescent nanoparticle	Ex (nm)	Em (nm)	Size (nm)	Detection method	Detection range	Limit of detection	Reference
H9N2 AIV	RuSi NPs	NA	NA	64 ± 3	ECL	25 fg/mL-25 ng/mL	14 fg/mL	[49]
Rabies virus	Ru@DMSNs	NA	612	242 ± 17	ECL	0.10 pg/mL-10 ng/mL	88 fg/mL	[51]
SARS-CoV-2	MB@AuNPs	633	NA	20 ± 6	SERRS	NA	0.046 ng/mL	[52]
SARS-CoV-2	$AIE_{810}NP$	680	810	310 ± 4	LFA	NA	IgM 0.236 μg/mL IgG 0.125 μg/mL	[19]
EV71 virus	TPE-APP	NA	NA	NA	Immunoassay platform	1.3×10^3-2.5×10^6 copies/μL	1.4 copies/μL	[59]
SARS-CoV-2	SWCNT	721	1130	NA	Optical sensing	0.005–5 pM	12.6 nM	[66]
Influenza A Influenza B	PS-NIR-II microspheres	750	1100	NA	LFA	NA	0.015 ng/m 0.037 ng/mL	[67]
HPV	AuNCs	NA	NA	NA	ECL	10^{-12}-10^{-8} M	0.48 pM	[96]
HBV	AuNCs	NA	NA	NA	ECL	0.1 pM-0.1 μM	0.1 fM	[97]
HIV	AuNCs	NA	NA	1.4 ± 0.3	ECL	0.1 fM-100 nM	30 aM	[99]
H5N1	AgNCs	NA	480	< 2	Fluorescent detection	500 pM-2 μM	500 pM	[20]
HPV	AgNCs	550 565	570 630	3	Ratiometric fluorescent	5 nM–100 nM	2 nM	[106]
SARS-CoV-2	CuNCs	NA	NA	NA	PCR	50 ng/μL-0.5 pg/μL	0.1 pg/μL	[110]
HBV	CuNCs	340	650	2.3	Fluorescent detection	0.5–100 pM	0.54 pM	[111]
SARS-CoV-2	LNPs	NA	615	NA	LFA	NA	NA	[21]
HBV	UCNPs	NA	540	67	LFA	0–10 nM	0.103 nM	[135]
AIV	UCNPs	980	800	30	LFA	$10^{1.49}$ EID_{50}/mL-$10^{5.37}$ EID_{50}/mL	H5N2: 10^2 EID_{50}/mL H5N6: $10^{3.5}$ EID_{50}/mL	[136]
H7N9	UCNPs	808	540	5	Fluorescent detection	100×10^{-12}-1×10^{-9} M	67 fM	[138]
Ebola virus	UCNPs	980	540	14	Fluorescent detection	50-700 fM	300 fM	[139]
H5N1	SWUCNPs	980	541	NA	Fluorescent detection	0.1–15 ng/mL	60.9 pg/mL	[140]
HPV16 HPV18	τλ-UCNPs	808	660 550 475	21.25 ± 0.83	Fluorescent detection	NA	NA	[143]
H1N1 H5N1 Adenovirus	UCNPs	980	550 470	30–40	Fluorescent detection	NA	NA	[145]
PRRSV	CdSe/ZnS QDs	NA	640	10	Fluorescent detection	10^1-3.5×10^4 $TCID_{50}$/mL	0.55 $TCID_{50}$/mL	[162]
Human Serum IgG	QBs	370	NA	NA	FLISA	0.005–40 ng/mL	4 pg/mL	[164]
IAV	MQBs	365	625	NA	LFA	NA	22 pfu/mL	[166]
SARS-CoV-2	QBs	NA	618	180	LFA	NA	NA	[168]
SARS-CoV-2 H1N1	SiTQD	NA	618	240	Immunochromatographic assay	0.01–100 ng/mL 100-10^5 pfu/mL	5 pg/mL 50 pfu/mL	[169]
SARS-CoV-2	QDMs	NA	NA	100	CFNS	NA	1 copy/mL	[22]
EBOV	ENs	NA	604	268 ± 8	ECL	0.02–30 ng/mL	5.2 pg/mL	[174]
HBV HCV	CdTe QDs	NA	551 607	NA	ECL	0.0005–0.5 nM 0.001–1.0 nM	0.082 pM 0.34 pM	[176]
SFTSV	CdTe@CdS QDs	NA	690	NA	ECL	0.01 fg/mL-100 pg/mL	0.0014 fg/mL	[177]
SARS-CoV-2	GPG	NA	NA	4.1	ULF NMR	0.5 fg/mL-5 μg/mL	0.5 fg mL	[181]
HIV HPV	CDs	NA	NA	< 5	ECL	100 fM–1 μM 1 pM–100 nM	30 fM 0.32 pM	[210]
HIV	CNPs	NA	NA	25–40	Fluorescent detection	1–50 nM	0.4 nM	[212]
HIV	CDs	350	461	3–4	Fluorescent detection	50.0 fM-1.0 nM	15 fM	[214]
HTLV-1	CDs	38	460	1.5	Fluorescent detection	10–320 nM	10 nM	[216]
SARS-CoV-2	MB-CDs	NA	NA	8	ECL	NA	2.00 aM	[219]
SARS-CoV-2	CDs	NA	NA	6.5 ± 0.5	ECL	NA	514 aM	[221]
HIV	BN-CDs	340	44	2.0–4.0	ECL	100 aM-1 nM	18.08 aM	[222]
SARS-CoV-2	CNDs	320	405	15	ECL	NA	1.2 pg/mL	[224]
Zika virus	FCS	NA	NA	NA	LFA	NA	10 pg/mL	[226]
SARS-CoV-2	RCS	580	634	1.1	LFA	NA	10 pg/mL	[227]
FAdVs	GQD	NA	405	20	Photoelectric sensor	NA	8.75 PFU/mL	[228]
HAV HBV	COFs	NA	NA	NA	Fluorescent detection	0.1–10 nM 0.5–10 nM	75 pM 150 pM	[229]
HIV	MOFs	NA	NA	NA	Fluorescent detection	NA	10 pM	[230]
ASFV	TRFNPs	NA	NA	NA	TRFIA	0.24–500 ng/mL	0.015 ng/mL	[232]

NA: Not available.

and near-infrared (NIR) dye-doped fluorescent nanoparticles (NIRFNs) (Fig. 4).

2.2.1. Conventional organic dye-doped fluorescent nanoparticles-based sensors

Conventional fluorescent dyes have certain drawbacks, such as low quantum yield, poor photostability, and photobleaching. Examples include fluorescein isothiocyanate (FITC), rhodamine b (RhB), and coumarin. Due to their chemical inertness, thermal stability, optical clarity, and superior biocompatibility, nanoparticles are the perfect carriers for organic fluorescent dyes and provide the possibility of addressing the aforementioned fundamental flaws of fluorescent dyes [45]. As shown in Fig. 4(a), silica nanoparticles (SNPs) [46], polystyrene nanoparticles [47], and MOFs [48] are often utilized carriers. The fluorescence signal of organic dye-doped fluorescent nanoparticles is substantially

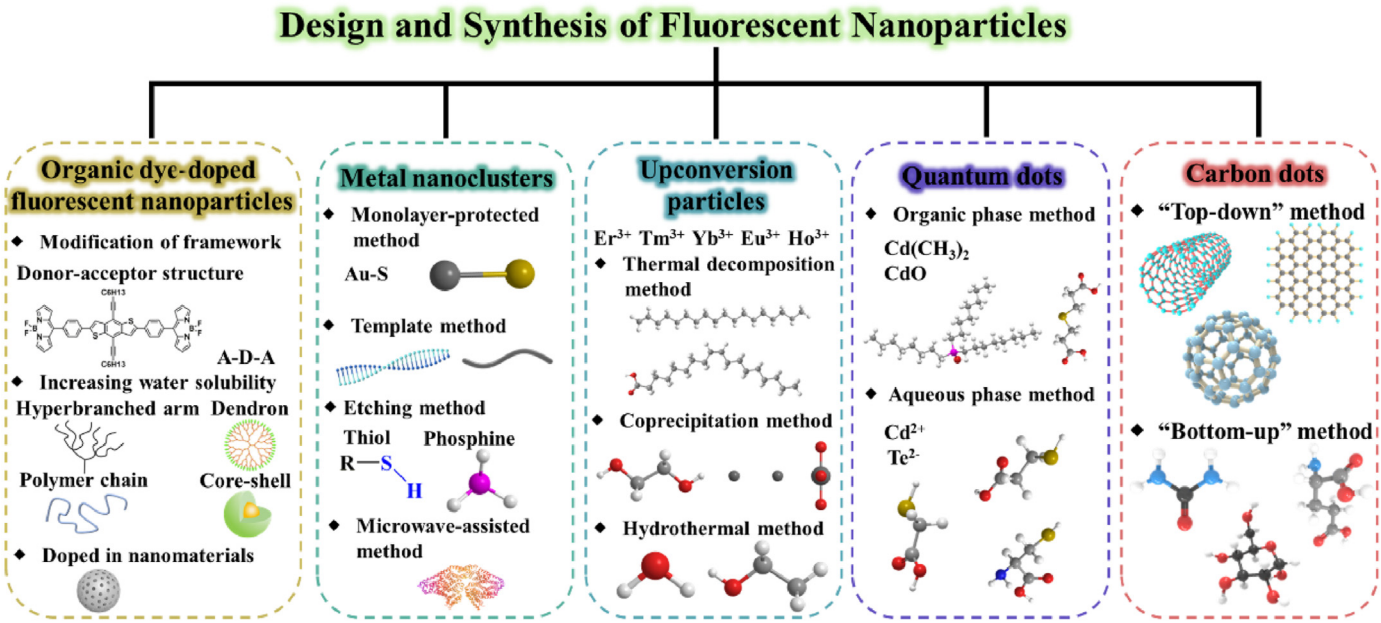

Fig. 3. The design of different fluorescent nanoparticles and their commonly used precursor materials.

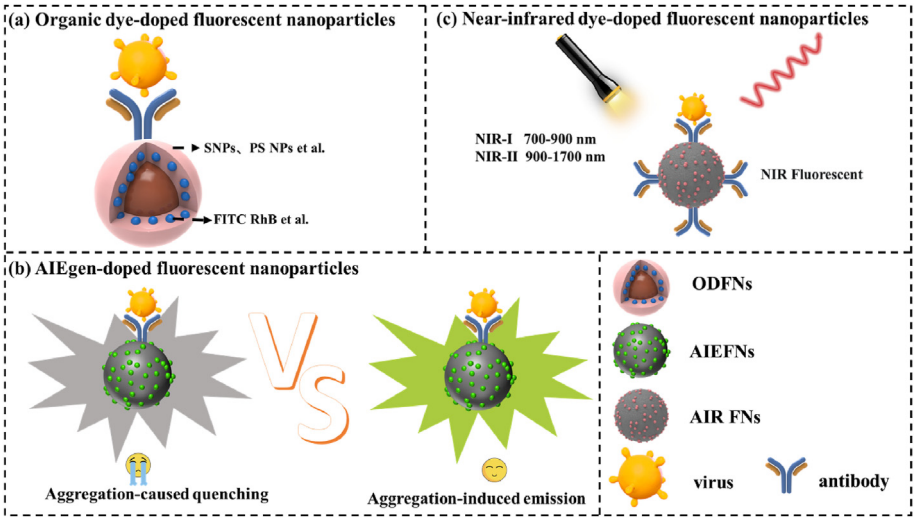

Fig. 4. The application of organic dye-doped fluorescent nanoparticles in virus detection. (a) organic dye-doped fluorescent nanoparticles, (b) AIEgen-doped fluorescent nanoparticles, (c) near-infrared dye-doped fluorescent nanoparticles.

improved and made possible by the integration of tenfold, hundredfold, thousandfold, or even ten-thousandfold organic fluorescent dyes in one nanomaterial, which allows the highly sensitive detection of the target. For example, Luo et al. successfully prepared functional silica nanospheres (RuSi NPs) by covering Ru $(BPY)_3^{2+}$ in silica nanoparticles. Compared to Ru $(BPY)_3^{2+}$, the same concentration of RuSi NPs could amplify Electrochemiluminescence (ECL) signals by about 10^3-fold, significantly improving the sensitivity. This RuSi NPs was used as an amplified fluorescent signal tag in combination with immunomagnetic separation (IMS) and electrochemical analysis to detect low abundance H9N2 AIV with a limit of detection (LOD) of 14 fg/mL [49]. In comparison to SNPs, dendritic mesoporous silica nanoparticles (DMSNs) can expose more active sites due to their open 3D dendritic shape and large specific surface area, which allows for easier access by other substances to the reaction and their participation. DMSNs doped with Ru $(BPY)_3^{2+}$ is used for the quantitative detection of rabies virus (RABV) with LOD as low as 88 fg/mL [50]. Additionally, the double signal mode, which uses ECL emissions as the first signal and DPV signals as the second signal, overcomes the drawback of the high false alarm rate of single signal output by increasing the precision and reliability of the detection [51]. For the detection of SARS-CoV-2, surface enhanced resonance raman scattering (SERRS) using methylene blue doped gold nanoparticles as a signal tag is superior to RT-PCR in terms of detection time, sensitivity, and convenience [52].

2.2.2. AIEgens-doped fluorescent nanoparticles-based sensors

Conventional organic fluorescent molecules are typically rigid planar molecules with large conjugation systems that can emit strong fluorescence in dilute solution. However, in high-concentration solutions or aggregated states, the fluorescence intensity of organic fluorescent dyes will be drastically reduced due

to strong intermolecular interaction (π-π stacking) [53] and large amounts of non-radiative deactivation, namely aggregation cause fluorescence quenching. Because of the aggregation-caused quenching (ACQ) effect of conventional organic fluorescent dyes, it is difficult to prevent the aggregation of fluorescent molecules in practical applications. This makes it difficult to design high-concentration cladding and organic dye-doped fluorescent nanoparticles [54]. It's interesting to note that in 2001, Prof. Ben-Zhong Tang's group discovered that silicon heterocyclopentadiene derivatives essentially exhibited no luminescence in diluted solution but displayed extremely bright fluorescence emission in the aggregated state, referring to this phenomenon as aggregation-induced emission (AIE) [55]. Because of their special molecular stacking mode, fluorescent dyes with AIE effect can reduce intermolecular interaction and inhibit the non-radiative inactivation process of single molecules, resulting in much higher fluorescence intensity in the solid state or aggregate state than in dilute solution. Therefore, AIEgens not only successfully solves the ACQ problem, but also has significant Stokes shift, excellent photostability, robust photobleaching resistance and high signal-to-noise ratio, which has considerable promise in the field of ultrasensitive virus detection (Fig. 4(b)). Currently, based on the exceptional features of AIEgens, it has now attracted the attention of researchers via a range of diverse synthesis techniques, including nanoprecipitation [56], microemulsion self-assembly [57], template expansion [19], and precipitation polymerization [58]. For example, Chen et al. used an organic solvent method to package the BPBT molecule into PS nanoparticles and combined with the lateral flow immunoassay (LFA), successfully detected SARS-CoV-2. More importantly, the AIE_{810}NP-based test strip can identify IgM or IgG 1−7 days after the onset of signs, whereas the AuNP-based strip cannot (8−15 days) [19]. Another water-soluble multifunctional AIEgen (TPE-APP) was degraded to TPE-DMA by the ALP enzyme, increasing the fluorescence intensity by 380 times. After antibody functionalization, the LOD for EV71 virus was 1.4 copies/μL. Unlike PCR, this approach does not necessitate extensive sample preparation or expensive instruments [59].

2.2.3. NIR dye-doped fluorescent nanoparticles-based sensors

Traditional fluorescence sensors display excitation or emission spectra in the ultraviolet to the visible light range. However, detection findings in this range may be disturbed by background signals from biological samples, such as light scattering [60]. However, biological samples typically display ultra-low NIR fluorescence signals (NIR I 700−900 nm, NIR II 900−1700 nm) [61−64]. In contrast to short-wavelength dyes, NIR dyes with longer emission wavelengths have a high signal-to-noise ratio, which can effectively reduce interference from light scattering from biological materials and improve detection sensitivity [65]. Therefore, NIR dye-doped fluorescent nanoparticles are an outstanding assay for detecting viruses in Fig. 4(c). Based on non-photobleaching and ease of functionalization, single-stranded carbon nanotubes (SWCNTs) can be minimally absorbed and scattered by biomolecules in the field of NIR dye-doped fluorescent nanoparticles, which has proven to be extremely useful in bioanalyte sensing. Furthermore, SWCNTs can be easily integrated into portable morphofactors to detect near-infrared SWCNT signals using Raspberry PI and charge-coupled device camera systems, which are shaped similarly to cellphones. Pinals et al. employed SWCNTs as signal transducers and demonstrated a 73% fluorescence on-off response within 5 s after being exposed to 35 mg/L SARS-CoV-2 virus-like particles, achieving a rapid and label-free detection of SARS-CoV-2 Spike Protein [66]. In principle, increasing the number of NIR dye-radiative radiations for a single target or replacing gold nanoparticles (AuNPs) with a new fluorescence signal reporter are both viable ways to boost LFA sensitivity. A highly sensitive NIR-based LFA platform that encapsulates a second near-infrared (NIR-II) fluorescent dye in polystyrene (PS) nanoparticles and integrates it into a lateral flow detection platform for quantitative detection of influenza A/B was recently developed, with LODs of 0.015 ng/mL and 0.037 ng/mL, respectively. The sensitivity of this strip is approximately 16 times that of the Au-based lateral flow test strip, and the stability is good [67].

3. Metal nanoclusters

Metal nanoclusters (MNCs) are made up of metal atoms and ligands and have a size that corresponds to the electronic Fermi wavelength. They are becoming more popular in the production of nanomaterials due to their ultra-small size (≤2 nm) [68], outstanding photophysical characteristics, strong biocompatibility, and huge specific surface area [69,70]. However, due to its poor QY, it did not initially attract the interest of researchers. In recent years, novel techniques for manufacturing metal nanoclusters, particularly metal (Au, Ag, Cu, etc.) nanoclusters, have been developed [71]. Metal nanoclusters have tunable fluorescence and are easier to manufacture than conventional organic dyes, making them more promising in the field of virus detection. Therefore, in this section, we focus on MNCs synthesis methods and its application in virus detection.

3.1. Preparation and synthesis

The preparation techniques of metal nanoclusters determine the diversity of sizes and properties that are directly related to the particle size, morphology, and internal structure of the particles. The template method (also known as the ligand-preserving method), monolayer-protected method, and others (chemical reduction method, seed growth method, ultrasonic method, microwave method, and chemical etching method) are some of the preparation techniques that are accessible [72−74]. The primary synthetic techniques will be discussed in this section (Fig. 3).

3.1.1. Template method

The template method is also one of the synthesis methods of metal nanoclusters, which are further classified as Thiolate-protected MNCs [75], Polymer-protected MNCs [76], Proteins or enzymes-protected MNCs [77], DNA-protected MNCs [78,79], and so on. Varied types of templates can give different spatial stereoscopic structures or functional chains, resulting in metal nanocluster surface functionalization. Thiolate-protected MNCs are based on the strong affinity of sulfur atoms in sulfhydryl compounds for metals such as gold, silver, and copper. Yin et al. rapidly obtained aqueous thiolated Ag@Au nanoclusters with a QY of ~18% (~12 min) [75]. Isozaki et al. prepared gold nanoclusters (AuNCs) functionalized with peptide dendritic thiolate ligands to form hydrogen-bonded supramolecular reaction fields [80]. Polymers are also commonly used as ligands containing a large number of charged and hydrophobic groups, such as polyethyleneimine (PEI), chitosan, polyvinylpyrrolidone (PVP), and so on. Nakal-Chidiac et al. synthesized silver nanoclusters protected by chitosan-containing polyamine moieties. Chitosan provides a polydentate macromolecular scaffold for the clusters, which can reproducibly and controllably stabilize the silver nanoclusters in aqueous media [81]. Zhou et al. prepared PEI-protected silver nanoclusters using formaldehyde as a reducing agent. Compared with thiol ligands, PEI, a branched polymer, has multiple interactions with metal nuclei, improving the stability of the clusters [82]. Proteins or enzyme-protected MNCs have an advantage over other methods in that they are easy to synthesize, usually using one-pot and “green”

synthesis methods. It has been demonstrated that AuNCs co-functionalized by two proteins of different sizes exhibit considerably greater fluorescence intensity than AuNCs stabilized by a single protein [83]. Based on this, gold nanoclusters with intense red fluorescence and high stability were quickly created using bovine serum albumin (BSA), lysozyme (LYZ), and $HAuCl_4$ [84]. Besides, other protein molecules such as papain [85] and pepsin [86] were also used as ligands to prepare metal nanoclusters. Furthermore, DNA-protected MNCs can change the wavelength of fluorescence emission and the particle size of nanoclusters by changing the sequence of nucleotides. The production of NIR-emitting DNA-stabilized silver nanoclusters (DNA-AgNCs), with an extraordinarily high fluorescence QY, was proposed by Neacsu et al. [87]. Additionally, Chai et al. synthesized poly-thymidine single-stranded protected fluorescent copper nanoclusters for label-free and cost-free detection of H_2O_2 in serum samples [88].

3.1.2. Monolayer-protected method

The monolayer-protection method refers to MNCs that have a particular function and may be created by layering molecules on their surface. Thiols often include −SH, which easily attaches to metals via metal-sulfur bonds (M − S), generating more stable metal nanoclusters. When these metals encounter thiol compounds in solution, the sulfur atoms in the thiol compounds form coordination bonds with the metal, generating a monomolecular layer with a passivation-like effect on the metal surface. Therefore, sulfhydryl compounds are commonly used as ligands to protect metal nanoclusters [89,90]. Doping gold into an unstable copper nanocluster (a glutathione-capped bimetallic copper), CuAuNCs@GSH, increased the photoluminescence stabilization duration to 7 days and yielded a quantum yield of 22% [91].

3.1.3. Other methods

Aside from the methods described above, there are various methods to synthesize MNCs. For instance, the chemical etching method has caught the interest of researchers due to its capacity to sculpt nanomaterials at the atomic level [92]. By using thiol-induced chemical etching, Shu et al. created oligomer shells for silver nanoclusters of the AIE type that showed enhanced water storage stability (over 3 months) [93]. Unfortunately, some research has indicated that the QY of MNCs made via chemical etching is unsatisfactory [94]. Unlike chemical etching, the microwave-assisted method has received a lot of praise for enhancing the efficiency of nanomaterials production because of its unique benefits of consistent heating, low energy consumption, cost-effectiveness, and environmental friendliness [74]. The microwave-assisted method, which is frequently used to reduce reaction times, uses electromagnetic fields to speed up chemical processes and raise system temperature. Yue et al. employed BSA as a reducing and stabilizing agent to manufacture high-fluorescence AuNCs with 16 gold atoms by microwave-assisted method and control the microwave power to shorten the reaction time from several hours to 1 h [72].

3.2. Application of virus detection

Metal nanoclusters are effective probes for fluorescence and chromaticity signals due to their outstanding fluorescence and catalytic characteristics [69]. Similarly, the interaction of metal nanoclusters with analytes might generate changes in the metal core, ligand shell layer, or surrounding microenvironment, resulting in property changes. Consequently, metal nanoclusters act as both recognition elements and signal conversion elements, providing excellent selectivity and sensitivity for virus detection. Nowadays, metal nanoclusters such as gold nanoclusters (AuNCs), silver nanoclusters (AgNCs), and copper nanoclusters (CuNCs) have been widely produced and have obtained excellent achievements in the fields of biomarkers, biosensing, bioimaging, and bioassays [71]. This section concentrates on the usage of the three metal nanoclusters mentioned above in the field of virus detection (Fig. 5).

3.2.1. AuNCs-based sensors

AuNCs have superior electrical characteristics in comparison to AgNCs and CuNCs, which have become more popular in the field of ECL. As illustrated in Fig. 5(a), Liu et al. developed a Cas12a-based ECL biosensor employing L-methionine-stable gold nanoclusters (Met-AuNCs) as effective ECL emitters to detect human papilloma virus (HPV) with a LOD of 0.48 pM, significantly lower than prior research [95], and the detection can be completed within 70 min [96]. The AuNCs-based electrochemical impedance biosensor can detect hepatitis B virus (HBV) in serum with great sensitivity, no label, and a low LOD of 0.1Fm, and the sensor's relative standard deviation (RSD) was as low as 1.39%, demonstrating strong repeatability and reproducibility [97]. However, the materials employed as templates for nanoclusters, such as BSA, glutathione (GSH), polyamylamine dendrimers (PAMAM), or DNA, are often non-conductive and restrict the delivery of electrical biosensors [83,84]. Research has shown that AuNCs and graphene hybrids have increased the electrocatalytic activity and stability of redox processes [98]. Wang et al. effectively identified human immunodeficiency virus (HIV) with a LOD of 30 aM using a one-step synthesis of graphene stabilized AuNCs (GR/AuNC) paired with an electrochemical biosensor [99].

3.2.2. AgNCs-based sensors

AgNCs have stronger fluorescence than AuNCs and CuNCs, which have the same stable ligands. For instance, the red fluorescent dihydrolipoic acid stabilized Ag NCs (DHLA-AgNCs) (QY: 3.3%) [100] are brighter than both DHLA-AuNCs (QY: 2.9%) [101] and DHLA-CuNCs (QY:2.8%) [102]. Owing to their relatively simple conformation, precise chemical recognition characteristics, and customizable sequence structures, DNA oligonucleotides are good scaffolds for the manufacture of metal nanoclusters. AgNCs prepared with DNA as a template not only has good photostability, biocompatibility, and high QY, but they also maintains the molecular recognition function and efficiently avoids complex labeling [103]. C-rich DNA is the most suitable template for AgNCs synthesis [104]. Zhang et al. developed a new label-free fluorescence sensing technology for H5N1 virus detection based on DNA template silver nanoclusters (DNA-AgNCs), with a LOD of 500 pM, the insertion of a three-segment branching DNA structure with a C-rich loop resulted in brilliant fluorescence and a wide range (500 pM-2 μM) of H5N1 detection [20]. Following the formation of nanocluster dimer (NCD) with another AgNCs, the fluorescence of AgNCs is either improved or shifted. The distance between two AgNCs or the changeover between dimer and non-dimer might affect the intensity or hue of the fluorescence [105]. Using C-rich DNA templates, Yan et al. created fluorescent Probe 1-AgNCs and non-fluorescent Probe 2-AgNCs that produced bright yellow and weak red, respectively. The primary fluorescence color of AgNCs shifted from yellow to red when HPV-16 DNA was hybridized with ProBe1-AgNCs and ProBe2-AgNCs to form NCD, enabling the ratio detection of HPV. Based on this, it can detect HPV in human serum with a LOD of 2 nM and a detection range of 5 nM−100 nM [106].

3.2.3. CuNCs-based sensors

CuNCs exhibit higher biocompatibility, less toxicity, and good cost performance in contrast to AuNCs and AgNCs [107]. More importantly, by varying the amounts of A/T base pairs, it is possible

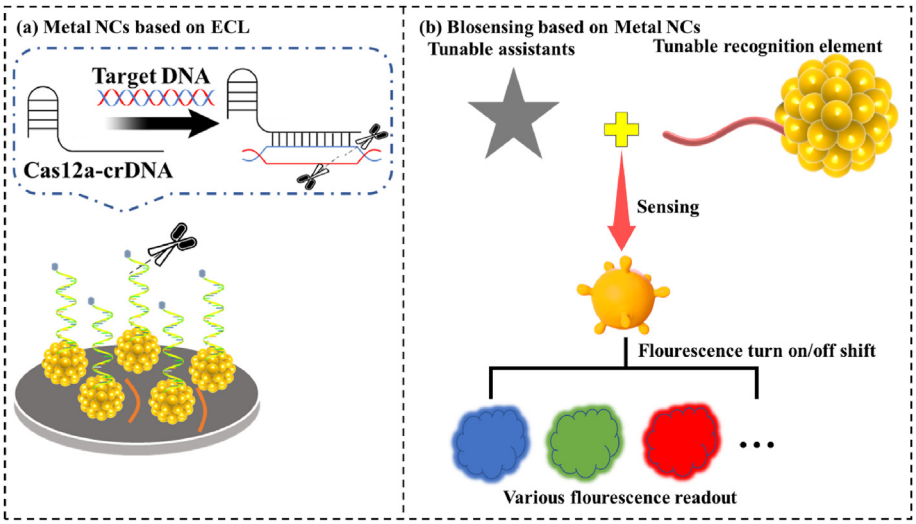

Fig. 5. The application of metal nanoclusters in virus detection. (a) Metal NCs based on ECL, (b) Blosensing based on Metal NCs.

to advantageously regulate the size and fluorescence intensity of CuNCs [108,109]. Additionally, various properties of copper ions and copper nanoclusters can be used to modify the luminescence state of the sensor devices (Fig. 5(b)). Du et al. created CuNCs using AT-rich primers as a template to identify the SARS-CoV-2 Delta virus via PCR. This approach not only distinguishes single nucleotide deletion virus from wild-type coronavirus, but it also allows for precise visualization [110]. Interestingly, researchers have compared the sensitivity of different metal nanoclusters to luminescent nanoprobes. They combined AuNCs, AgNCs, and CuNCs made with DNA as a template with the CRISPR-Cas12a enzyme to create a fluorescence biosensor for HBV detection. The CuNCs-based nanosensor was discovered to be more sensitive (AuNCs: 162.41 pM, AgNCs: 78.24 pM and CuNCs: 0.54 pM). Moreover, the fluorescence response of CuNCs to HBV detection was much quicker (AuNCs: 12 h, AgNCs: 2 h, and CuNCs: 25 min) [111].

4. Up-conversion nanoparticles

Up-conversion nanoparticles (UCNPs) can transform low-energy photons into high-energy photons by adhering to the anti-Stokes luminescence law. UCNPs have the advantages of strong signal penetration, no background fluorescence interference, good photostability, and easy surface modification that are significantly better than conventional fluorescent dyes [112,113], and have been widely used as an excellent fluorescent signal output element in the fields of sensing detection and medical imaging. The synthesis methods of UCNPs and their applications in virus detection will be the main topics of discussion in this section.

4.1. Synthetic methods

Typical up-conversion luminous materials may be divided into three primary categories: triplet-triplet annihilation (TTA) based up-conversion nanomaterials [114], rare-earth doped (RED) up-conversion nanomaterials [115] and two-photon absorption (TPA) up-conversion nanomaterials [116]. Among them, rare-earth doped up-conversion luminescence (UCL), which is currently the most effective and widely used UCL system, primarily exploits the energy transfer between lanthanide rare earth ions (such as Yb^{3+} and Er^{3+}) to create up-conversion luminescence. UCNPs are typically produced using one of three methods: co-precipitation, hydrothermal, or thermal degradation. This section will describe the above synthetic methods in detail (Fig. 3).

4.1.1. Thermal decomposition method

Thermal decomposition method is the dissociation of organometallic precursors (e.g., acetate, trifluoroacetate) by heating at high temperature in a high boiling point organic solvent medium. Generally, the organic solvent is high boiling point octadecene (ODE), and the surface inert ligands in the reaction system are oleamine (OM) and oleic acid (OA), which chelate with the released lanthanide ions to control the formation of nanocrystals [117]. Therefore, to prepare high-performance UCNPs, it is crucial to choose the suitable precursors, ligands, control of the nucleation and development phases. To produce high-quality UCNPs, Ye et al. used a thermal decomposition method with CF_3COONa and $RE(CF_3COO)_3$ as precursors to prepare UCNPs in various shapes (spheres, rods, hexagonal prisms, and plates) by varying the reaction duration and sodium to lanthanum trifluoroacetate ratio [118]. Many researchers have refined the synthesis conditions and created more advanced materials because of this pioneering effort [119,120]. However, the yield of UCNPs was only around 100 mg, which was inadequate. You et al. prepared $NaYF_4$ UCNPs by solid-liquid thermal decomposition, after adjusting the reaction temperature and adding the amount of CH_3COONa, the yield of UCNPs with different sizes and phases reached 67 g [121]. Although the thermal decomposition method is frequently employed, it produces poisonous compounds (such as HF, oxyfluorocarbon, and so on) during the preparation process, which is harmful to human health.

4.1.2. Coprecipitation method

To avoid the fatal shortcoming of thermal decomposition method, researchers sought a gentler method of preparing UCNPs, and the coprecipitation method was born. The coprecipitation method involves adding the precipitant to a soluble salt solution containing a range of ions, causing all the ions to precipitate out the insoluble products, and then washing and heating to obtain nanomaterials. The synthesis process is simple to use, and the instrument is inexpensive. Stephen et al. utilized coprecipitation to synthesize UCNPs with 1-adamantanecarboxylic acid as the ligand [122]. Yi et al. created NaYF4: Yb, Er UCNPs ethylene diamine tetraacetic acid (EDTA) as the ligand without using pyrolysis [123]. However, none of them succeeded in producing UCNPs with

homogeneous shape and size. To solve this issue, Li et al. used a moderate coprecipitation method to generate β-NaYF4: Yb, Er and β-NaYF4: Yb, Er series UCNPs. To achieve high-quality and uniformly dispersed UCNPs, this method included the precipitation of amorphous UCNPs formed at ambient temperature prior to incubation at high temperature [124]. This strategy has now become one of the most popular methods for synthesizing UCNPs [125,126].

4.1.3. Hydrothermal method

As we all know, water is a fantastic solvent for a wide range of chemicals, including acids, bases, salts, ionic complexes, and so on. Nevertheless, due to high temperature environment required for the nucleation process, water has a low boiling point and is not the best solvent for the synthesis for UCNPs. Since the boiling point of water increases with pressure, the researchers have designed the hydrothermal method, in which water or organic solvents are used as the reaction medium to generate high temperature and pressure by heating in a closed vessel (such as a autoclave), and then the reactants undergo various chemical reactions to produce dispersed nanomaterials [127]. For instance, Wu et al. used a straightforward, one-step hydrothermal method to produce homogenous, almost spherical $AgBi(MoO_4)_2$-based phosphor particles without the need for a surfactant [128]. It has also been proposed to use hydrothermal synthesis to create very homogenous UCNPs of various shapes (from the tube, plate, and rod, to highly complicated flower-like structures) [129]. Adding low-boiling solvents like cyclohexane or methanol can also effectively alter the size of UCNPs. Furthermore, other UCNPs have been synthesized using this method [130,131].

4.2. Application of virus detection

Based on the following benefits, up-conversion fluorescence technology is becoming more and more popular in areas such as environmental monitoring, biomarkers analysis, medication therapy, food detection, etc. To begin with, UCNPs have high photostability, are not easily accepted by the external environment (such as acidity and temperature), do not contain harmful chemicals, and have negligible toxicity to cells. Secondly, UCNPs are emitted by low-energy excitation and high-energy emission, which can prevent the detection process from being hampered by the sample's background spontaneous fluorescence and increasing detection sensitivity. Thirdly, UCNPs are dimmable, and by varying the kind and percentage of doping elements, fixed wavelength excitation and multi-band emission can be obtained. Fourthly, excitation light is a near-infrared light source with excellent tissue penetration. Up-conversion nanomaterials detect viruses primarily using fluorescent tagging, energy transfer, and two-dimensional encoding (Fig. 6).

4.2.1. Fluorescent labeling

Compared with traditional fluorescent materials, UCNPs are a new class of fluorescent materials that can overcome the disadvantage of fluorescence background interference, light scattering of traditional fluorescent detection and become one of the best fluorescent markers due to their special up-conversion luminescence properties. In particular, Fig. 6(a) shows the basic principle of LFA detection, which is a simple, disposable, and affordable diagnostic tool that may be optimal for the rapid and accurate identification of certain viral infectious diseases [132]. When combined with UCNPs, LFA provides excellent photostability, enhanced signal-to-noise ratio, and highly sensitive detection of various samples [133]. Chen et al. used LFA to detect SARV-CoV-2 IgG using lanthanide-doped polystyrene nanoparticles (LNPs) as a signal label. The complete test takes about 10 min, suggesting that it might be a quick and easy immunodiagnostic technique for COVID-19 to supplement the gold standard method [21]. In general, static imaging UCNP-LFA can better satisfy POCT requirements, particularly when combined with information and tiny devices, such smart phones [134]. Gong et al. created a tiny portable HBV detection platform employing an LFA detection device, a UCNP-LFA reader, and a smart phone. The LOD was as low as 0.103 nM, which was approximately 5−10 times lower than the clinical cut-off value [135]. To pursue a lower LOD, Kim et al. designed an LFA platform for identifying the Avian influenza virus (AIV) using NIR to NIR up-conversion. The addition of Ca^{2+} increased the up-conversion photoluminescence (PL) emission peak intensity of UCNPs, allowing for the detection of AIV within 20 min, with a LOD that was ten times lower than that of the commercially available GNP-based AIV LFA [136].

4.2.2. Energy transfer

Fluorescence resonance energy transfer (FRET) is a non-radiative energy transfer process based on donor-acceptor dipole interactions. The excited donor transfers energy to the acceptor before returning to the ground state. The acceptor accepts energy and produces certain changes in the surrounding electrons, resulting in the FL signal changing. FRET-based sensor designs typically need to meet the following requirements: (1) the distance between the donor and acceptor must be smaller than 10 nm. (2) the donor's emission spectrum must overlap with the acceptor's absorption spectrum [137]. Unfortunately, FRET-based sensors are disturbed by background fluorescence interference, which affects the detection accuracy. The up-conversion function of UCNPs compensates for this shortcoming. Consequently, researchers prefer UCNPs-based FRET sensors with two main modes, turn on and turn off (Figure (6b)). AuNPs are often used as fluorescence receptors due to their superior extinction coefficient and good photostability. A FRET sandwich assay for the detection of H7N9 was devised, with up-converted nanoparticles and gold nanoparticles serving as donors and acceptors, respectively. The hybridization time is roughly 40 min, making it particularly attractive for application in field-based fast influenza screening [138]. The same researchers have previously suggested heterogeneous analysis of UCNPs and AuNPs using the nanoporous alumina (NAAO) solid-phase technology to detect the Ebola virus at the femtomolar level [139]. However, the size of the UCNPs is a critical component in this system to assure the fluorescence effect. UCNPs, which are sandwich structures created via a layer-by-layer seed-mediated shell growth strategy, can increase signal intensity. Based on π-π stacking between the aptamer and GO, the sensor is successfully implemented for H5N1 detection [140].

4.2.3. Two-dimensional encoding

With the development of detection technology, the method that can only detect one analyte at a time has limited its application because of the high consumption of reagents and specimens. High-throughput multiplex coding is a powerful tool for virus diagnosis by simultaneously detecting and identifying multiple analytes in a single sample with minimal volume [141]. The two primary categories of spectral coding based on UCNPs are the time domain and frequency domain in Fig. 6(c). While maintaining the same crystal structure and shape, varied doping ion concentrations can produce nanoparticles with varying lifetimes that are less influenced by ambient background, differing collecting efficiency, and other factors [142]. By creating a core/multi-shell structure, adjusting the emission color, and regulating the decay lifetime of UCNPs, the time-resolved imaging scanning system comprising a spectrometer and a time-correlated single photon counting (TCSPC) coupled fluorescence microscope can successfully distinguish between HPV16 and HPV18. Compared to the traditional color/intensity

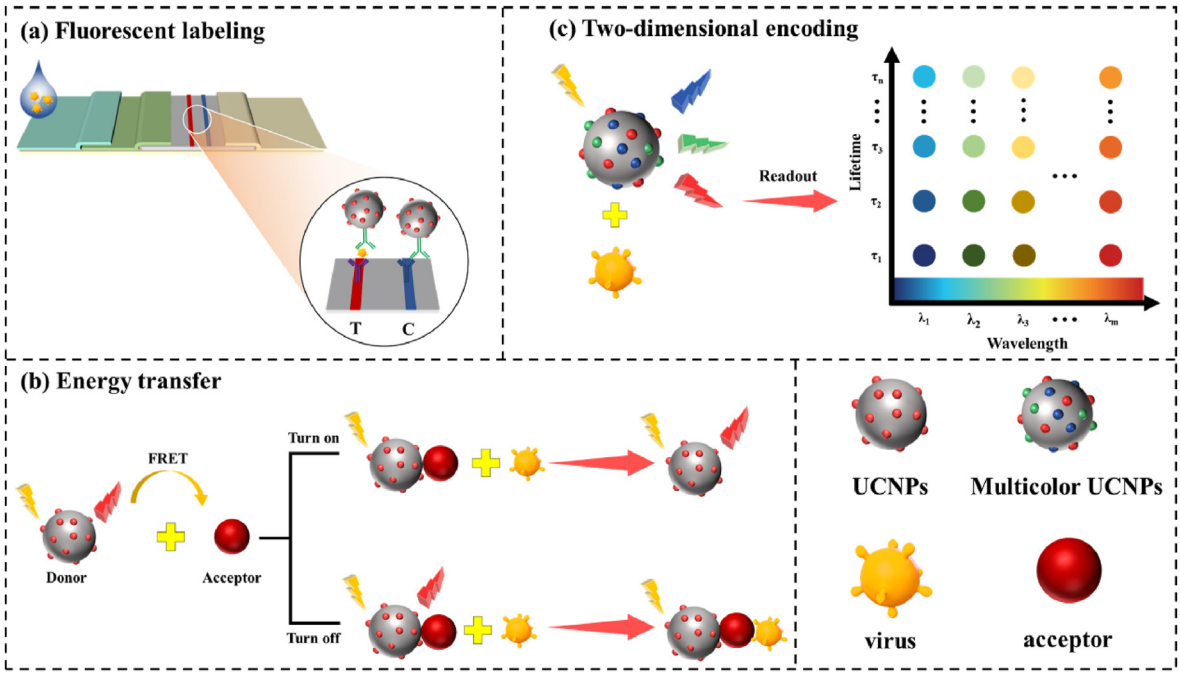

Fig. 6. The application of up-conversion particles in virus detection. (a) fluorescent labeling, (b) energy transfer, (c) two-dimensional encoding.

methods, this novel color/lifetime binary scheme has exponentially scalable encoding capacities (>10^5) and is three orders of magnitude better than traditional methods [143]. Similarly, using the frequency domain as a coding dimension is also useful in detection [144]. It is possible to simultaneously identify and detect serum IgG and IgM antibodies against the human adenovirus and influenza A virus by using the distinctive green and blue emission bands of Er and Tm doped UCNPs [145].

5. Quantum dots

Quantum dots (QDs), also known as semiconductor quantum dots, are nanocrystals made up of inorganic nuclei and organic molecules that cover the nucleus's surface. They are mostly constituted of II-VI, III-V, and IV-VI elements, with particle sizes ranging from 1 to 10 nm [146]. QDs' superior performance compensates for the absence of conventional organic dyes, such as high fluorescence quantum yield, broad excitation peak tunable emission, superior photostability, and diverse surface modification [147]. Because of their excellent optical properties, QDs can be used as a good fluorescent signal label in detection [148], biological imaging [147], optical devices [149], and other fields. In this section, we focus on the synthesis methods of QDs and their application in virus detection.

5.1. Synthetic methods

The synthesis of QDs is the fundamental requirement for their use, and different synthesis methods can lead to changes in the shape and properties of QDs, which can affect their subsequent application. Therefore, researching how to manufacture QDs with excellent quality and quantum yield is critical for future application research. At present, QD synthesis methods are mostly classified into two methods: organic phase synthesis and water phase synthesis (Fig. 3).

5.1.1. Organic phase synthesis

Organic phase synthesis is the process of rapidly pyrolyzing a precursor in a high boiling point organic solvent under high-temperature conditions, followed by gradual development to QDs of the chosen size. This method was first proposed by Bawendi et al., who successfully prepared CdE (E = S, Se, Te) QDs with good dispersion and crystallization using dimethyl cadmium ($Cd(CH_3)_2$) as the precursor and trioctylphosphine/trioctylphosphine oxide (TOP/TOPO) as the ligand solvent, but the QY was pessimistic [150]. Furthermore, several research groups enclosed QDs in shells, which not only preserved the QDs' unique optical properties but also increased the QY [151]. However, the major weakness of QDs made with Cd $(CH_3)_2$ as the precursor is that they are extremely poisonous. Subsequently, some researchers proposed using CdO, which is less hazardous, as the precursor for the green synthesis of quantum dots in place of $Cd(CH_3)_2$. This method is more reliable and straightforward than $Cd(CH_3)_2$-related systems [152]. With the in-depth research of QDs synthesis method, the prerequisite materials of organic phase synthesis are expanded from group II-VI to group III-V and group IV-VI, and from single-type QDs to tetradic and doped QDs [153,154]. The development of these new QDs increases the variety of QDs available, enhances their functionality, satisfies research demands, and broadens the scope of applications for QDs.

5.1.2. Aqueous phase synthesis

Compared with organic phase synthesis, aqueous phase synthesis has the advantages of low cost, low toxicity, simple operation, and green security. To obtain good water solubility, biocompatibility, and chemical stability of QDs, Weller et al. first applied aqueous phase synthesis method. Aqueous CdTe was synthesized by using Cd as the precursor and sulfhydryl compounds as the stabilizing agent. In this process, QDs with different particle sizes and characteristics can be obtained by regulating the concentration of precursor substances, the reference of Cd and Te, pH, etc [155]. Obviously, it is known that precise experimental parameter optimization is essential for enhancing QDs synthesis in

the aqueous phase. Studies have shown that polyacrylic acid (PAA) can interact strongly with CdTe nanoparticles via the coordination of carboxyl groups and cadmium ions on the particle surface. In other words, the acidic range improves the luminescence efficiency of CdTe nanoparticles stabilized by thiol carboxylic acid [156]. Since then, more and more people have further improved the water phase synthesis method and derived some new water phase synthesis methods for QDs, such as hydrothermal method [157], ultrasonic radiation method [158], and microwave radiation method [159]. Of these, hydrothermal method not only has all the advantages of aqueous phase synthesis method, but also shortens the synthesis time, reduces the surface defects of QDs and improves the luminescence of QDs, which has become the most popular method for QDs preparation.

5.2. Application of virus detection

Compared with conventional organic dyes, the fluorescence intensity and stability of QDs are 20 times and two orders of magnitude higher, respectively, which can improve the sensitivity of the method for probe labeling. Importantly, QDs are highly biocompatible and their surface may be chemically changed with antibodies, nucleic acids, and other macromolecules without affecting their biological capabilities, facilitating virus detection [160]. This section focuses on three mainstream applications of quantum dots in virus detection: Immune magnetic separation-QDs fluoroimmunoassay, QDs-based lateral flow assay, and QDs-based biosensors (Fig. 7).

5.2.1. Immune magnetic separation-QDs fluoroimmunoassay

As shown in Fig. 7(a), immune magnetic separation is a simple pretreatment method based on the interaction of antigen and antibody, which is characterized by excellent anti-interference ability, rapid speed, good stability, and can rapidly enrich the target from the complicated mechanism [161]. Combination with quantum dots enables virus detection and quantification. Based on immunomagnetic separation, a new FRET assay for the detection of Porcine reproductive and respiratory syndrome virus (PRRSV) was constructed using CdSe/ZnS as fluorescence donors and AuNPs as fluorescence receptors, which enable the detection of low concentrations of PRRSV in pig serum in a wide range (10^1-3.5×10^4 $TCID_{50}$/mL) [162]. However, in complicated samples, single QDs exhibit inadequate luminescence intensity and poor photostability. The stability and fluorescence intensity of quantum dot nanobeads (QBs) are substantially higher than those of quantum dots due to the doping of numerous quantum dots, which can significantly increase the sensitivity of the detection method [163]. Therefore, the fluorescent linked immunosorbent assay (FLISA) based on magnetic Fe_3O_4 nanospheres and QBs is an excellent choice for detecting IgG in human serum and may be expanded to detect SARS-CoV-2 specific IgM and IgG in serum [164]. Given the complementary advantages of QDs and magnetic nanoparticles (MNPs), magnetic quantum dot nanobeads (MQBs) composed of QDs and MNPs have been developed to achieve immune enrichment and fluorescent labeling [165]. Bai et al. constructed the LFA of MQBs for magnetic enrichment and fluorescence detection of Influenza A virus (IAV) in clinical specimens, with the LOD (22 pfu/mL) about 2200 times lower than that of traditional gold nanoparticle colorimetric LFA (5×10^4 pfu/mL) [166].

5.2.2. QDs-based lateral flow assay

Lateral flow assay is a well-established, straightforward, portable, affordable, and user-friendly technology that has become an ideal candidate for on-site virus detection in a variety of matrices. It is also widely used in food safety, supervision clinical diagnosis and other fields [167]. The following benefits make the LFA-based respiratory virus detection approach an excellent choice for enhancing SARS-CoV-2 infection detection: (i) without sample preparation processes, the approach may be used immediately on respiratory specimens, and results are quick (typically 10–20 min) and (ii) the LFA test strip is suited for quick viral screening of infected individuals and utilized in hospitals, communities, schools, and any other public locations. As shown in Fig. 7(b), for the detection of total SARS-CoV-2 antibodies in human serum, an LFA based on QBs synthesized with numerous quantum dots embedded in a polymer matrix (QB-LFA) was created. Compared with AuNPs-LFA, the proposed method's sensitivity is enhanced by almost an order of magnitude [168]. Following that, a similar method was described, in which the triple-QD shell (SiTQD) was used as a signal probe to construct a dual-channel platform for simultaneous

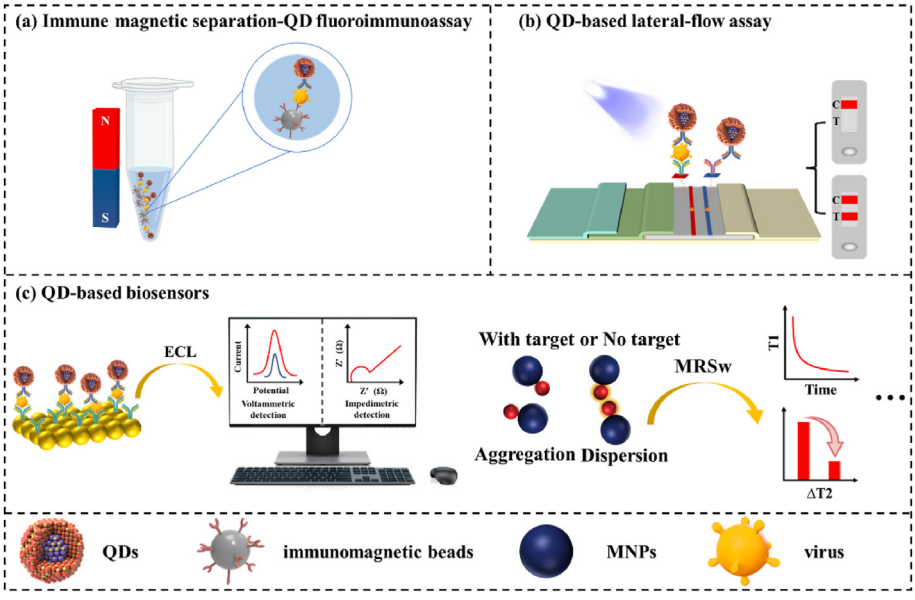

Fig. 7. The application of quantum dots in virus detection. (a) Immune magnetic separation-QD fluoroimmunoassay, (b) QD-based lateral-flow assay, (c) QD-based biosensors.

detection of SARS-CoV-2 and IVA (within 15 min), with the LOD as low as 5 pg/mL and 50 pfu/mL, respectively. The novel method improves the sensitivity of the standard AuNP-based LFA method by two orders of magnitude and is more sensitive than the prior method [169]. However, because of problems with sensitivity and cross-reactivity, serological testing can only be used as an adjuvant to the diagnosis of viral infections. Based on this, nucleic acid detection is still the method of choice for finding SARS-CoV-2, and several nucleic acid-based detection methods have been created. Zhang et al. first combined Cas13-based nucleic acid detection strips with quantum dot microspheres (QDMS) for the detection of SARS-CoV-2. The method costs less than $1.50 for a single test, and the fluorescent nanoprobes and nucleic acid test strips can be stored at room temperature for at least 3 months, which has the potential to be used in site-directed detection [22].

5.2.3. QDs-based biosensors

Biosensors are recognized by their molecular recognition and signal transduction abilities, which enable them to convert biochemical data into optical or electrical signals. Up to now, many biosensors have been proposed for virus detection, such as surface plasmon resonance (SPR) [170] and surface enhanced raman scattering (SERS) [171]. In addition to the methods mentioned above, ECL is a superior detection and analysis technique because of its high sensitivity, easy optical setup, strong temporal and spatial controllability, minimal background signal, and lack of a light source. QDs and ECL integration-based detection methods have attracted a lot of interest since Bard et al. published their initial study on the ECL of Si QDs in 2002 [172]. However, the effectiveness of ECL based on quantum dots is rather low when compared to conventional ECL reagents, such as Ru $(BPY)_3^{2+}$ and luminol, which restricts the practical applicability [173]. As a result, signal amplification strategies are required to increase detection sensitivity. Currently, as shown in Fig. 7(c), signal amplification methods are classified into three types: (1) loading QDs on carrier materials with a high specific surface area or with a robust carrier structure (silica nanoparticles, carbon nanomaterials, metal-organic skeletons, etc.). An amount of CdSe/ZnS QDs was embedded into copolymer nanospheres by simple ultrasound to produce uniform electroluminescent nanospheres (ENs). On this basis, MNPs were combined for ultrasensitive EBOV detection, which could detect EBOV as low as 5.2 pg/mL in 2 h [174]. (2) using co-reactive catalysts (solid metal alloys, oxides, and novel nanoparticles) to speed up the formation of free radicals. It has been demonstrated that H_2O_2 and $K_2S_2O_8$ double coreactants can increase ECL strength by more than 100-fold [175]. Liu et al. employed $K_2S_2O_8$ to increase the intensity of ECL and constructed an electrochemical sensor based on the fluorescent internal filtering effect between CdTe QDs and gold nanoparticles (AuNPs) for the detection of hepatitis B and C viruses, with LOD of 0.082 pmol/L and 0.34 pmol/L, respectively [176]. (3) using an effective matrix for indirect signal amplification. Photonic crystal (PC) is a novel form of microstructure material in which materials with varying dielectric constants are placed in a periodic pattern. Because of its light collecting and light amplification properties, PC is frequently employed to increase biosensor signals. Because the electrode modified with SiO_2 photonic crystal nanofilm could successfully boost the ECL strength by nearly 7-fold, an enhanced NIR-ECL biosensor with the LOD as low as 0.0014 fg/mL was constructed for ultrasensitive SFTSV diagnosis [177]. However, in the above method, the tube must be opened during testing, which may result in aerosol contamination and further virus spread. Consequently, avoiding opening the test tube during the testing process to prevent aerosol contamination can effectively reduce the risk of infection of testing personnel. Fig. 7(c) shows mgnetic relaxation switch (MRSw) based on the nuclear magnetic resonance (NMR) phenomenon can be applied to biomarker detection, significantly simplifying detection steps, realizing closed-loop detection, and achieving low background and high simplicity sensing [178]. Recent research has shown that the Gd^{3+} probe can improve MRSw sensitivity [179]. Meanwhile, ultra-low field (ULF) NMR can double the relaxation of Gd^{3+} complexes compared to 1.5 T, which is beneficial to biomarker identification [180]. In the ULF NMR method, Gd^{3+} loaded polyethylene glycol (PEG) modified GQDs (GPG) was employed to detect SARS-CoV-2 pseudovirus, which the detection time was less than 2 min and the total cost of a single GPG test is only $1.25 [181]. Even though numerous QDs-based biosensors for virus detection have been established, they have not yet been fully commercialized, most likely because the LOD has not yet reached an acceptable level, or the repeatability and stability of the method still need to be improved. To satisfy the demands for detection, researchers must improve biosensors that are more reliable, portable, fast, and environmentally friendly.

6. Carbon dots

Carbon dots (CDs) are zero-dimensional fluorescent carbon nanostructures with particle sizes of 10 nm [182]. CDs have many unmatched advantages over conventional heavy metal quantum dots and organic dyes, including low cost and low environmental impact synthesis, a straightforward synthesis route, a variety of fluorescence characteristics, better water solubility, good biocompatibility, and strong resistance to photobleaching [183]. CDs with different forms have distinct names due to their complicated structure and great variation, primarily graphene quantum dots (GQDs) and carbon quantum dots (CQDs). Furthermore, the surface of CDs is rich in hydroxyl, carboxyl, carbonyl, and epoxy groups, making carbon quantum dots easier to functionalize and expanding the application spectrum of carbon quantum dots [184]. CDs combine the optical capabilities of quantum dots with the physicochemical properties of carbon nanomaterials to provide greater benefits [185]. Consequently, CDs research has been involved in biomedicine, environmental pollution detection, and photocatalysis, and has achieved outstanding results. In this section, we will focus on the synthesis methods of CDs and the application of virus detection.

6.1. The synthetic methods

To date, various synthetic methods have been described to synthesize CDs with varying physical and chemical characteristics, which may be readily tuned by modifying reaction variables such as feedstock, temperature, pH, and so on. The available synthetic methods for CDs are broadly classified as top-down method and bottom-up method (Fig. 3).

6.1.1. Top-down method

Top-down method refers to the cutting of larger precursors (such as graphene, activated carbon, carbon nanotubes, etc.) into small-sized nanomaterials by physical or chemical methods, such as arc discharge method, laser etching method, electrochemical oxidation method, etc., which the principle of preparation is primarily the large size of carbon material decomposed into micron, eventually forming carbon quantum dots. CDs were first discovered using arc discharge method when researchers discovered fluorescent carbon materials in the process of purifying single-walled carbon nanotubes produced by arc discharge soot [186]. However, the CDs obtained by arc discharge method are generally complex in composition and have low QY [187]. Surface passivation is one of the most effective methods for increasing QY. Sun et al. developed a

two-step procedure for manufacturing high CDs with a QY close to 60% employing PEG_{1500N} (passivating agents, help in the generation of fluorescence by introducing surface defects and they provide active sites for further modifications) as a surface passivator based on this finding [188]. Similarly, using graphene oxide (GO) and low-cost commercial activated carbon as carbon sources, HNO_3 as an oxidant, and amine-terminal compounds as surface passivation, Shen [189] and Qiao [190] et al. combined chemical oxidation and surface functionalization to make CDs with high QY. Although the above method produces CDs with excellent QY, the operation is laborious, the yield is poor, and the PL is not changeable. After that, Peng [191] and Liu [192] et al. manufactured CDs by oxidative cutting using carbon fibers (CFs) as carbon sources. More importantly, by varying the reaction temperature, the emission wavelength of CDs may be controlled. To decrease costs, coal has also been used to chemically oxidize carbon to create CDs. By varying the coal's oxidation cutting conditions or graphite crystal structure, CDs size and optical qualities may be changed [193]. The laser ablation method can directly synthesize CDs without additional passivation by carefully selecting the appropriate carbon target or its medium, which attracts the attention of researchers. To bypass the time-consuming preparatory procedure, a one-step laser ablation technique was developed by optimizing the experimental conditions. The graphite powder dispersed in PEG200 N was irradiated with a Nd: YAG laser for 2 h while being assisted by ultrasound, and the synthesis and surface modification happened concurrently to produce CDs with a QY of 5% [194]. Contrarily, Yu et al. avoided the usage of passivation agents like PEG by synthesizing CDs instead of bulk carbon materials by using toluene as a carbon precursor [195]. The laser ablation technique has the advantages of being simple to use and having a variable PL. However, the method has some inherent difficulties such as low yield, short wavelength of CDs, expensive equipment, and few applications. Fortunately, Li et al. generated a series of CDs with size-dependent PL by varying the current intensity of the base aided electrochemical system, resulting in a color shift from blue to brown with sizes ranging from 1.2 to 3.8 nm [196]. In contrast to the methods mentioned above, the electrochemical synthesis method has been widely employed since it is easy to use, and the equipment is easily accessible, which generally uses carbon materials with good conductivity as the working electrode and carbon sources. After a certain voltage is applied, the oxidation reaction takes place in the anode, thereby shedding the CDs on the carbon source. In 2007, Sham first used this method to synthesize blue CDs with a QY of 6.4%, which used multiwalled CNTs (MWCNTs)-covered carbon paper as the working electrode and carbon source, a Pt wire as the counter electrode, $Ag/AgClO_4$ as a reference electrode, and tetrabutylammonium perchlorate (TBAP)-containing acetonitrile solution as the electrolyte [197]. Later then, the researchers achieved the electrochemical preparation of CDs by switching to a more cost-effective carbon source, such as petroleum coke and graphite rod [198,199]. Furthermore, Li et al. obtained three GQDs with different optical properties by electrochemical oxidation using aqueous phosphate buffer solution, aqueous NaOH solution and aqueous KCl solution as electrolytes, respectively, verifying that changing the electrolyte can affect the morphology and fluorescence properties of GQDs [200]. However, top-down electrochemical synthesis has been criticized for its low QY. Inspired by the bottom-up method, proposed a facile bottom-up preparation strategy of CDs by electrochemical carbonization of ILs-containing nitriles as both parameters and carbon sources, which provide new ideas for the improvement of electrochemical methods [201].

6.1.2. Bottom-up method

Bottom-up method primarily employs tiny molecules containing carbon as precursors (sucrose, citric acid, glucose, and so on) to self-assemble CDs, which the most often utilized methods include hydrothermal methods, pyrolysis methods, microwave methods, and so on. Compared with the top-down method, the proposed method showed high QY and strong photoluminescence intensity [202]. Hydrothermal method is the most efficient way to synthesize CDs, which is primarily a carbonization process at quite a high temperature and pressure. Small molecule precursors are more beneficial in the hydrothermal synthesis of CDs. The tiny molecule L-ascorbic acid was processed for 4 h at 180 °C in a combination of deionized water and ethanol to create homogeneously and scattered blue luminous CDs, but the QY was lower (6.79%) [203]. On the other hand, under the same hydrothermal synthesis conditions, nitrogen-containing CDs from chitin and chitosan exhibited greater QY and bigger sizes than nitrogen-free CDs from glucose, demonstrating significant effects on the QY and morphology of CDs [204]. Besides, using citric acid and ethylenediamine (EDA) as carbon and nitrogen sources, respectively, blue luminous CDs with a QY of 80% and a high output of 58% were synthesized, demonstrating that the modification of CDs with heteroatoms could effectively change its physical and chemical properties, particularly enhance QY [205]. The hydrothermal method is simple to use, offers a diverse variety of carbon sources, and does not demand the use of specialized equipment. More significantly, CDs with multicolor emission may be made by adjusting the reaction conditions, which is beneficial for biomedicine, sensing, optoelectronics, and other applications. Pyrolysis method, which is separated into liquid phase pyrolysis and solid phase pyrolysis, is another method for producing CDs with high QY. Wang et al. used pyrolysis for the first time to create high QY (53%) oil-soluble CDs with varying properties by carbonizing anhydrous citric acid (carbon precursor) in a hot mixture of uncoordinated solvent octadecene and surface passivator 1-hexadecylamine at 300 °C by varying the reaction solvent or reaction time [206]. Subsequently, Pan et al. devised a one-step solid-phase pyrolysis process for producing high-blue luminous CDs with QYs ranging from 31.6 to 40.6% without the need for any solvent [207]. This method can obtain CDs with high QY, but it is difficult to obtain uniform CDs due to the cumbersome process. In particular, it is difficult to prepare long-wavelength CDs by pyrolysis method, which greatly limits the application of CDs. Unlike hydrothermal and pyrolytic methods, the microwave method can reduce reaction time to a few minutes, allowing for the quick production of CDs. By employing the microwave method and inexpensive citric acid and urea as carbon and nitrogen, respectively, N-doped CDs with QY up to 14% were created [208]. Later on, the QY of N-doped CDs rose to 40.2% when EDA was employed as a nitrogen source instead of urea [209]. This method has the potential for extensive industrialization since it is more time-efficient and cost-effective.

6.2. Application of virus detection

As previously mentioned, CDs have a variety of interesting properties, including good stability, simplicity of surface modification, minimal cytotoxicity, and excellent biocompatibility [185]. Researchers have given CDs a lot of consideration as viable candidate material for biosensing. In recent years, virus detection has seen significant efforts and advances. Appropriate incorporation of CDs as a significant component of viral genome detection techniques appears to increase viral identification sensitivity and specificity. Therefore, this section makes an appropriate summary based on the optical sensors, electrochemical sensors, lateral flow assays, and microfluidic analysis of CDs (Fig. 8).

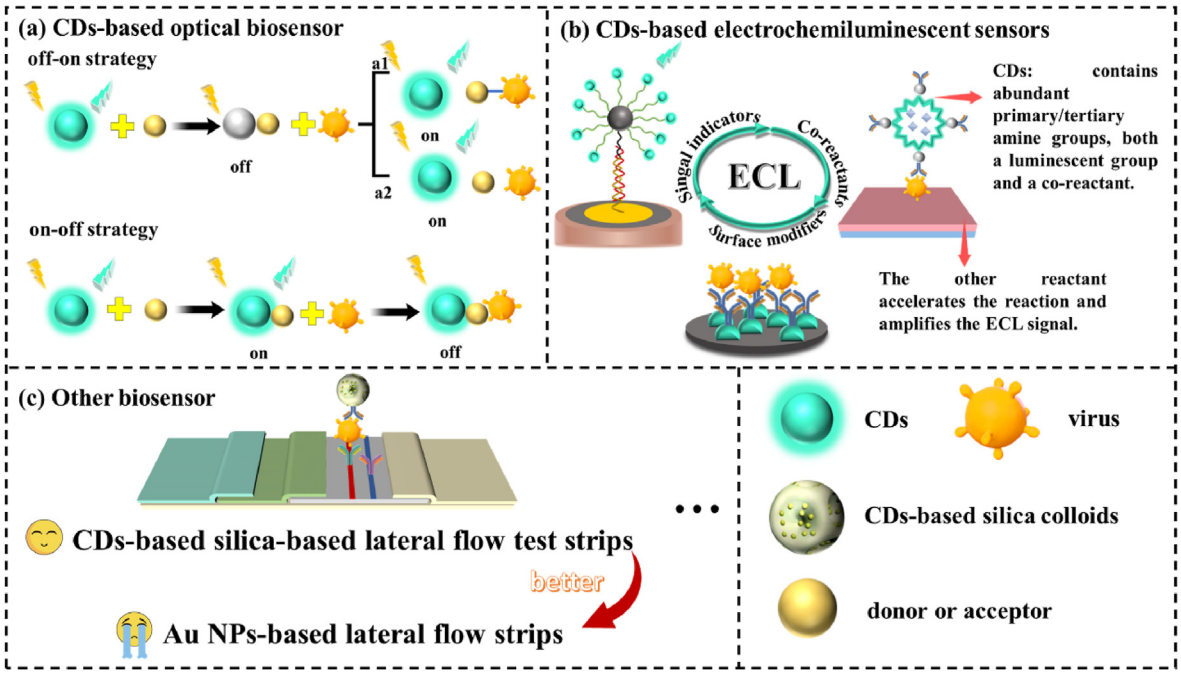

Fig. 8. The application of carbon dots in virus detection. (a) CDs-based optical biosensor, (b) CDs-based electrochemiluminescent sensors, (c) Other biosensors.

6.2.1. CDs-based optical sensors

Combining optical discs with technological tools can result in accurate, quick, and sensitive virus identification. CDs can operate as energy donors or acceptors and have variable elemental compositions, converting optical changes into measurable signals like fluorescence intensity, colorimetric wavelength, or longevity. This allows us to categorize optical sensors based on CDs into two major groups in Fig. 8(a): on-off and off-on. On the one hand, the on-off strategy, namely fluorescence quenching, is the most typical sensing design for CDs-based optical sensors, and this technique has been used to detect a variety of cations, anions, tiny compounds, pathogenic bacteria, and viruses. Zhao et al. designed an electrochemiluminescence biosensor with an "on-off" signal for the dual detection of HIV and HPV. Namely, the biosensor was incubated with HIV DNA and CDs-labeled SNA ECL luminescence mass before obtaining the "on" ECL signal. To acquire the "off" ECL signal, the biosensor was incubated with helper DNA, CDs-labeled SNA, and Cas12a/crRNA/HPV-16 dsDNA complex. The benefit of this method is that it can perform equivalent detection in under 2 h without the need for extra nucleic acid amplification stages or numerous Cas protein effectors [210]. On the other hand, the off-on strategy enables the measurement of the analyte concentration by bringing the quenched CDs back to the emission state. For FRET-based biosensing, a variety of carbon-based materials are frequently utilized because of their almost ubiquitous, long-range, and highly efficient photoluminescence quenching characteristics. Due to their significant light absorption windows, CNPs have distinguished themselves as superior materials for use as energy acceptors [211]. CNPs were used as the fluorescence acceptor and two-probe fluorescent AgNCs as the fluorescence donor in the construction of a FRET-free biosensor for HIV detection, in which the LOD was 0.40 nM [212]. Graphene is also a promising substrate for the immobilization of inorganic nanoparticles. The combination of 2D GO with zero-dimensional AuNPs produces AuNPs/GO nanohybrids that not only combine the qualities of each component but also have fascinating structures and properties that the individual components do not have [213]. Inspired by this, a FRET-based HIV detection platform was developed using hydrothermal production of CDs of uniform size and AuNPs/GO composites as quenches. This approach offers substantially higher selectivity and sensitivity for detecting HIV gene-related DNA in the femtomole concentration range than the previously published method [214]. In recent years, MNPs have been quickly produced and have had a revolutionary influence on food safety, environmental monitoring, biomedicine, and other fields [215]. Another study found that adsorption of the CDs-probe on the surface of Fe_3O_4@Au in the absence of a target reduced CDs fluorescence emission, which was recovered in the presence of the target because double-stranded DNA could not be adsorbed on Fe_3O_4@Au. The detection of Human T-lymphotropic virus type 1 (HTLV-1) was made possible as a result of this [216].

6.2.2. CDs-based electrochemical sensors

Electrochemical detection system has the advantage of fast response, high sensitivity, simple setup, wide detection range, flexibility, low cost, and compact structure [217]. Compared with other analysis methods based on optics, ECL has some incomparable advantages. One is that ECL does not need an external light source for light emission. In other words, there is no background signal for sample fluorescence. Secondly, the ECL emission can be controlled by the potential on the electrode. Thirdly, some of the ECL reactants can be electrochemically regenerated on the electrode, which greatly improves the detection sensitivity. Therefore, the integration of CDs into this assay technology and its integration into composite nanomaterials can increase the detection limit and thus integrate point-of-care devices into personalized medicine. CDs-based electrochemical sensors have three main mechanisms in Fig. 8(b): signal indicators, co-reactants, and surface modifiers. Although the ECL mechanism of CDs is not completely understood, there is evidence that the intensity of CDs luminescence is directly connected to its surface condition. Firstly, a novel synthetic approach is now being developed that enhances the ability to integrate certain groups into nanostructured carbon-dimensional networks and endows them with specified functionality. For

example, M. Prato et al. have shown how to choose appropriate precursors for CDs production by introducing particular electroactive groups into carbon dot nanostructures and changing their electrical and electrochemical characteristics [218]. In particular, an electrochemical indicator of methylene blue (MB) functionalized CDs paired with gold nanostructures of various shapes was synthesized to establish a sensing platform for SARS-CoV-2 detection with a detection limit as low as 2.00 aM [219]. Secondly, Co-reaction mechanisms have been created, such as the CDs-$S_2O_8^{2-}$, CDs-SO_3^{2-}, and CDs-SO_4^{2-} systems, which can improve the ECL response and sensing sensitivity of CDs by encouraging the creation of an initiator [220]. For example, CDs synthesized using a green chemical method were utilized as a co-reactive agent of $[Ru(BPY)_3]^{2+}$ anodic electrochemiluminescence, and SARS-CoV-2 was identified by a change in ECL signal when $[Ru(BPY)_3]^{2+}$/CDs was mixed with AuNMs nanostructures [221]. Similarly, Guo et al. developed a new triadic ECL system for ultrasensitive HBV-DNA detection by accelerating the co-reactant $S_2O_8^{2-}$-with boron and nitrogen co-doped CDs (BN-CDs) and platinum nanoflower (Pt NFs). which the detection ranges from 100 aM to 1 nM [222]. Thirdly, CDs are perfectly suited for usage as electrode surface modifiers due to their large surface area features. However, the conductivity of CDs is lower than that of common metals, which restricts the passage of electrode current. As a result, CDs are frequently mixed in certain composites to boost electrical conductivity and improve adsorption characteristics [223]. Guerrero-esteban et al. modified electrodes with synthetic nitrogen-rich CNDs (rich in aromatic primary amines) and utilized them as antibody carriers and ECL amplifiers to detect SARS-CoV-2 along a wide range, effectively applying them to SARS-CoV-2 detection in rivers and municipal wastes [224].

6.2.3. Other sensors

In addition to the above applications, CDs also plays an important role in lateral flow assay and fluorescence probe. Among the various biosensor platforms, paper-based biosensors are commercially attractive alternatives due to their simple preparation, ease of operation, availability, and transportability, coupled with low cost and efficient manufacturing, thus outperforming screen-printed glass carbon-based electrodes [225]. Lateral flow assays do not require complex instrumentation, but their sensitivity is often criticized. Commercial test strips generally use gold nanoparticles as signal reporters, but it has been shown that the LOD of silanized CDs-based LFA is lower than that of AuNPs-based LFA in Fig. 8 (c). Combining fluorescent CDs-based silica (FCS) colloids with LFA platform achieved the LOD as low as 10 pg/mL for the Zika virus, which is 100 times lower than AuNPs-based LFA [226]. Later on, a similar technique using red emission enhanced CDs-based silica (RCS) with a sensitivity of 10 pg/mL was employed to detect SARS-Cov-2. Once more, this approach has the potential to be employed in the future as a fresh, affordable, and straightforward detection tool, particularly in underdeveloped nations [227]. In addition, the photoelectric sensor is a rapid diagnostic tool that can provide accurate, reliable, field-portable low-cost equipment for practical applications. For example, Ahmed et al. reported a photoelectric sensor for fowl adenoviruses (FAdVs) detection that enhanced the local electric field through the interaction of GQD with gold nanobundles (AuNBs) to achieve highly sensitive detection, which is 100 times more sensitive than conventional ELISA methods [228].

7. Others

In addition to the five more frequent kinds of fluorescent nanoparticles described above, other advanced fluorescent nanomaterials, such as organic frameworks and time-resolved fluorescence nanoparticles (TRFNPs), have been broadly acknowledged as the choice for virus-sensing applications. The organic framework mainly includes covalent organic frameworks (COFs) and MOFs. COFs are porous polymer nanostructures with exceptional heat stability and density. However, COFs have only been employed once for virus identification due to the scarcity of high-energy electrons. In one research, COFs were combined with AuNPs and DNA that had been tagged with an Ag nanocluster to detect HAV and HBV [229]. In contrast, MOFs are the most commonly employed organic nanomaterials for virus detection. MOFs are coordination polymers with large specific surface areas, high porosity, fluorescence quenching, high loading efficiency, and tunable porosity that are primarily made of organic linkers and inorganic metals. The quenching performance of planar MOFs is superior to that of stereo MOFs due to their planar structure with the extensively exposed surface, rich functional groups, metal ions (positive charge), and huge conjugate system. Importantly, planar ligands may also lessen the MOFs steric hindrance, which would promote probe adsorption and hybridization. Zhao et al. created a variety of new water stable Zn^{2+} pterionic MOFs with the LOD of 10 pM for the selective and sensitive detection of HIV sequences. Compound 2 (Zn^{2+} and $Cbdcp^{2-}$) had the highest quenching performance due to its adequate pore size and planar shape [230]. Time-resolved fluorescence immunoassay (TRFIA) is a revolutionary detection method that uses the unique fluorescence features of lanthanides and offers greater sensitivity, reduced matrix interference, and a broader dynamic range than ELISA [231]. Chen et al. developed a TRFIA approach that uses a double antibody sandwich to detect African swine fever (ASFV) antigen which has equivalent performance to currently available ELISA assays [232]. Besides, there are other fluorescent nanoparticles in the detection field. For example, persistent luminescence nanoparticles (PLNPs) absorb the energy of ultraviolet, visible, near infrared and X-ray light and store it in lattice defects. When the excitation light goes out, the energy from the light source is slowly released and the light source continues to shine for seconds, hours, or days [233]. This continuous near-infrared light significantly reduces biological tissue self-fluorescence, effectively improves sensitivity and signal-to-noise ratio, and causes PLNPs to have a longer lifetime and stronger photostability than lanthanide fluorescent particles, making them highly potential probes [234]. However, no evidence of PLNPs being used in virus detection has been discovered. The study of PLNPs-based sensors is still in its early stages, and the creation of monodisperse and high-luminescence PLNPs has a lot of unexplored territories.

8. Conclusions and future perspectives

Due to the current global spread of viruses such as SARS-CoV-2 and monkeypox, there is an urgent need to improve the accuracy, sensitivity, specificity, and speed of virus detection. Also, there is an interest in developing alternative methods to conventional virus detection systems (e.g., PCR, ELISA). Fluorescent nanotechnology has great potential for rapid virus detection and identification, genomic analysis, and serological studies. The incorporation of nanomaterials provides multiple benefits for improved performance of viral sensors, such as increased sensitivity, specificity, and response time. On the one hand, in terms of the current state of application of fluorescent sensors for virus detection, the method has long been widely used, such as the FDA-approved fluorescence-based real-time reverse transcription polymerase reaction technique and the fluorescence-based immunochromatographic method for SARS-Cov-2 detection. On the other hand, in terms of the current state of fluorescent sensor virus detection machines, QPCR instruments are commonly used for the rest of the laboratory

for the quantitative detection of viruses, and antigen detection kits are more suitable for home screening. In addition, ECL, high-throughput multiplex coding and MRSw have also been developed. In this work, we discuss various methods of synthesis of fluorescent nanoparticles and recent developments in the applications of virus detection. Despite the development of fluorescent biosensors in the field of detection, there are still many issues and challenges that need to be addressed.

Firstly, the optical properties of fluorescent nanoparticles determine their analytical performance. The development of fluorescent nano biosensors needs to consider issues such as background fluorescence, fluorescence stability, and phototoxicity. In addition, issues such as toxicity and reproducibility of the biosensor should be addressed. Therefore, the synthesis of fluorescent nanoparticles must be further optimized to give high quantum yield, optical stability, low toxicity, and good dispersion of fluorescent nanoparticles by green synthesis methods.

Secondly, since viruses have a certain incubation period and are highly transmissible, coupled with the movement of people which expands their transmission range, on-site screening of viruses generally requires advantages such as high throughput, portability, and short detection time. However, most of the existing reported fluorescent biosensors are not suitable for in situ detection. Therefore, incorporating nanosensors into an affordable paper strip or smartphone system expands the range of “guaranteed” criteria (affordable, sensitive, specific, user-friendly, rapid, device-free, and delivered to the end-user) for nanomaterials for POCT of viral pathogens. This will not only improve the efficiency of the test analysis but also reduce the cost of the test and save manpower.

Finally, from the development of advanced fluorescent nanomaterials, near-infrared fluorescent materials with longer emission wavelengths can effectively shield complex biological matrices (e.g., biological proteins and pigments) from background interference and improve the accuracy of actual sample analysis. By coupling with other fluorescent materials to create dual-emission ratio fluorescent probes, built-in calibration can be provided to reduce systematic errors from the instrument and environmental effects, improve the signal-to-noise ratio, and make the platform suitable for commercialization.

CRediT authorship contribution statement

Qian Xu: Conceptualization, Writing-Original draft preparation, Software. Fangbin Xiao: Data curation, Visualization, Writing-Reviewing and Editing. Hengyi Xu: Writing- Reviewing and Editing, Project administration, Funding acquisition, Supervision.

Declaration of competing interest

The authors declare that they have no known competing financial interests or personal relationships that could have appeared to influence the work reported in this paper.

Data availability

No data was used for the research described in the article.

Acknowledgments

The work was supported by the National Key R&D Program of China (2018YFC1602500).

References

[1] N. Zhang, L. Wang, X. Deng, R. Liang, M. Su, C. He, L. Hu, Y. Su, J. Ren, F. Yu, L. Du, S. Jiang, Recent advances in the detection of respiratory virus infection in humans, J. Med. Virol. 92 (2020) 408.
[2] F. Zhou, T. Yu, R. Du, G. Fan, Y. Liu, Z. Liu, J. Xiang, Y. Wang, B. Song, X. Gu, L. Guan, Y. Wei, H. Li, X. Wu, J. Xu, S. Tu, Y. Zhang, H. Chen, B. Cao, Clinical course and risk factors for mortality of adult inpatients with COVID-19 in Wuhan, China: a retrospective cohort study, Lancet 395 (2020) 1054.
[3] L. Xu, J. Liu, M. Lu, D. Yang, X. Zheng, Liver injury during highly pathogenic human coronavirus infections, Liver Int. 40 (2020) 998.
[4] B. Anesten, A. Yilmaz, L. Hagberg, H. Zetterberg, S. Nilsson, B.J. Brew, D. Fuchs, R.W. Price, M. Gisslen, Blood-brain barrier integrity, intrathecal immunoactivation, and neuronal injury in HIV, Neurol. Neuroimmunol. Neuroinflamm 3 (2016), e300.
[5] A. Leligdowicz, W.A. Fischer, T.M. Uyeki, T.E. Fletcher, N.K.J. Adhikari, G. Portella, F. Lamontagne, C. Clement, S.T. Jacob, L. Rubinson, A. Vanderschuren, J. Hajek, S. Murthy, M. Ferri, I. Crozier, E. Ibrahima, M.-C. Lamah, J.S. Schieffelin, D. Brett-Major, D.G. Bausch, N. Shindo, A.K. Chan, T. O'Dempsey, S. Mishra, M. Jacobs, S. Dickson, G.M. Lyon, R.A. Fowler, Ebola virus disease and critical illness, Crit. Care 20 (2016).
[6] A.A. Dawood, Mutated COVID-19 may foretell a great risk for mankind in the future, New Microbes and New Infections 35 (2020).
[7] T. Thanh Le, Z. Andreadakis, A. Kumar, R. Gomez Roman, S. Tollefsen, M. Saville, S. Mayhew, The COVID-19 vaccine development landscape, Nat. Rev. Drug Discov. 19 (2020) 305.
[8] C. Liu, Q. Zhou, Y. Li, L.V. Garner, S.P. Watkins, L.J. Carter, J. Smoot, A.C. Gregg, A.D. Daniels, S. Jervey, D. Albaiu, Research and development on therapeutic agents and vaccines for COVID-19 and related human coronavirus diseases, ACS Cent. Sci. 6 (2020) 315.
[9] F. Wolters, J. van de Bovenkamp, B. van den Bosch, S. van den Brink, M. Broeders, N.H. Chung, B. Favié, G. Goderski, J. Kuijpers, I. Overdevest, J. Rahamat-Langedoen, L. Wijsman, W.J.G. Melchers, A. Meijer, Multi-center evaluation of cepheid xpert® xpress SARS-CoV-2 point-of-care test during the SARS-CoV-2 pandemic, J. Clin. Virol. 128 (2020).
[10] Z. Huang, D. Tian, Y. Liu, Z. Lin, C.J. Lyon, W. Lai, D. Fusco, A. Drouin, X. Yin, T. Hu, B. Ning, Ultra-sensitive and high-throughput CRISPR-p owered COVID-19 diagnosis, Biosens. Bioelectron. 164 (2020).
[11] J.C. Lownik, G.W. Way, J.S. Farrar, R.K. Martin, Extraction-free rapid cycle quantitative RT-PCR and extreme RT-PCR for SARS-CoV-2 virus detection, J. Mol. Diagn. 23 (2021) 1671.
[12] L. Chen, F. Ruan, Y. Sun, H. Chen, M. Liu, J. Zhou, K. Qin, Establishment of sandwich ELISA for detecting the H7 subtype influenza A virus, J. Med. Virol. 91 (2019) 1168.
[13] F. Watzinger, K. Ebner, T. Lion, Detection and monitoring of virus infections by real-time PCR, Mol. Aspect. Med. 27 (2006) 254.
[14] R.M. Lequin, Enzyme immunoassay (EIA)/enzyme-linked immunosorbent assay (ELISA), Clin. Chem. 51 (2005) 2415.
[15] J.R. Choi, Development of point-of-care biosensors for COVID-19, Front. Chem. 8 (2020).
[16] G. Mao, Y. Li, G. Wu, S. Ye, S. Cao, W. Zhao, J. Lu, J. Dai, Y. Ma, Construction of ratiometric Si-Mn:ZnSe nanoparticles for the immunoassay of SARS-CoV-2 spike protein, Sens. Actuators B Chem. 369 (2022), 132306.
[17] Z. Tang, X. Zhang, Y. Shu, M. Guo, H. Zhang, W. Tao, Insights from nanotechnology in COVID-19 treatment, Nano Today 36 (2021), 101019.
[18] A. Mokhtarzadeh, R. Eivazzadeh-Keihan, P. Pashazadeh, M. Hejazi, N. Gharaatifar, M. Hasanzadeh, B. Baradaran, M. de la Guardia, Nanomaterial-based biosensors for detection of pathogenic virus, Trends Analyt Chem. 97 (2017) 445.
[19] R. Chen, C. Ren, M. Liu, X. Ge, M. Qu, X. Zhou, M. Liang, Y. Liu, F. Li, Early detection of SARS-CoV-2 seroconversion in humans with aggregation-induced near-infrared emission nanoparticle-labeled lateral flow immunoassay, ACS Nano 15 (2021) 8996.
[20] Y. Zhang, F. Mu, Y. Duan, Q. Li, Y. Pan, H. Du, P. He, X. Shen, Z. Luo, C. Zhu, L. Wang, Label-free analysis of H5N1 virus based on three-segment branched DNA-templated fluorescent silver nanoclusters, ACS Appl. Mater. Interfaces 12 (2020), 48357.
[21] Z. Chen, Z. Zhang, X. Zhai, Y. Li, L. Lin, H. Zhao, L. Bian, P. Li, L. Yu, Y. Wu, G. Lin, Rapid and sensitive detection of anti-SARS-CoV-2 IgG, using lanthanide-doped nanoparticles-based lateral flow immunoassay, Anal. Chem. 92 (2020) 7226.
[22] Q. Zhang, J. Li, Y. Li, G. Tan, M. Sun, Y. Shan, Y. Zhang, X. Wang, K. Song, R. Shi, L. Huang, F. Liu, Y. Yi, X. Wu, SARS-CoV-2 detection using quantum dot fluorescence immunochromatography combined with isothermal amplification and CRISPR/Cas13a, Biosens. Bioelectron. 202 (2022), 113978.
[23] Y. Xue, C. Liu, G. Andrews, J. Wang, Y. Ge, Recent advances in carbon quantum dots for virus detection, as well as inhibition and treatment of viral infection, Nano Converg. 9 (2022) 15.
[24] C. Ji, Q. Gao, X. Dong, W. Yin, Z. Gu, Z. Gan, Y. Zhao, M. Yin, A size-reducible nanodrug with an aggregation-enhanced photodynamic effect for deep chemo-photodynamic therapy, Angew Chem. Int. Ed. Engl. 57 (2018), 11384.
[25] C. Ji, W. Cheng, Q. Yuan, K. Mullen, M. Yin, From dyestuff chemistry to cancer theranostics: the rise of rylenecarboximides, Acc. Chem. Res. 52 (2019) 2266.
[26] L. Liu, Z. Ruan, T. Li, P. Yuan, L. Yan, Near infrared imaging-guided photodynamic therapy under an extremely low energy of light by galactose targeted amphiphilic polypeptide micelle encapsulating BODIPY-Br_2, Biomater. Sci. 4 (2016) 1638.
[27] D. Cao, Z. Liu, P. Verwilst, S. Koo, P. Jangjili, J.S. Kim, W. Lin, Coumarin-based

small-molecule fluorescent chemosensors, Chem. Rev. 119 (2019), 10403.
[28] V.N. Mehta, M.L. Desai, H. Basu, R. Kumar Singhal, S.K. Kailasa, Recent developments on fluorescent hybrid nanomaterials for metal ions sensing and bioimaging applications: a review, J. Mol. Liq. 333 (2021).
[29] L. Jiao, Y. Liu, X. Zhang, G. Hong, J. Zheng, J. Cui, X. Peng, F. Song, Constructing a local hydrophobic cage in dye-doped fluorescent silica nanoparticles to enhance the photophysical properties, ACS Cent. Sci. 6 (2020) 747.
[30] W. Cheng, H. Chen, C. Liu, C. Ji, G. Ma, M. Yin, Functional organic dyes for health-related applications, View 1 (2020).
[31] Y. Cai, W. Si, W. Huang, P. Chen, J. Shao, X. Dong, Organic dye based nanoparticles for cancer phototheranostics, Small 14 (2018).
[32] G. Chen, I. Roy, C. Yang, P.N. Prasad, Nanochemistry and nanomedicine for nanoparticle-based diagnostics and therapy, Chem. Rev. 116 (2016) 2826.
[33] X. Gao, D. Mao, X. Zuo, F. Hu, J. Cao, P. Zhang, J.Z. Sun, J. Liu, B. Liu, B.Z. Tang, Specific targeting, imaging, and ablation of tumor-associated macrophages by theranostic mannose-AIEgen conjugates, Anal. Chem. 91 (2019) 6836.
[34] C. Chen, H. Ou, R. Liu, D. Ding, Regulating the photophysical property of organic/polymer optical agents for promoted cancer phototheranostics, Adv. Mater. 32 (2020), e1806331.
[35] B. He, Y. Chu, M. Yin, K. Müllen, C. An, J. Shen, Fluorescent nanoparticle delivered dsRNA toward genetic control of insect pests, Adv. Mater. 25 (2013) 4580.
[36] S. You, Q. Cai, Y. Zheng, B. He, J. Shen, W. Yang, M. Yin, Perylene-cored star-shaped polycations for fluorescent gene vectors and bioimaging, ACS Appl. Mater. Interfaces 6 (2014), 16327.
[37] M. Sun, W. Yin, X. Dong, W. Yang, Y. Zhao, M. Yin, Fluorescent supramolecular micelles for imaging-guided cancer therapy, Nanoscale 8 (2016) 5302.
[38] Y. Zheng, S. You, C. Ji, M. Yin, W. Yang, J. Shen, Development of an amino acid-functionalized fluorescent nanocarrier to deliver a toxin to kill insect pests, Adv. Mater. 28 (2016) 1375.
[39] M. Chen, M. Yin, Design and development of fluorescent nanostructures for bioimaging, Prog. Polym. Sci. 39 (2014) 365.
[40] F. Qiu, Q. Zhu, G. Tong, L. Zhu, D. Wang, D. Yan, X. Zhu, Highly fluorescent core−shell hybrid nanoparticles templated by a unimolecular star conjugated polymer for a biological tool, Chem. Commun. 48 (2012), 11954.
[41] W. Lin, Y. Li, W. Zhang, S. Liu, Z. Xie, X. Jing, Near-infrared polymeric nanoparticles with high content of cyanine for bimodal imaging and photothermal therapy, ACS Appl. Mater. Interfaces 8 (2016), 24426.
[42] R. Sauer, A. Turshatov, S. Baluschev, K. Landfester, One-pot production of fluorescent surface-labeled polymeric nanoparticles via miniemulsion polymerization with bodipy surfmers, Macromolecules 45 (2012) 3787.
[43] D. Wang, H. Wu, J. Zhou, P. Xu, C. Wang, R. Shi, H. Wang, H. Wang, Z. Guo, Q. Chen, In situ one-pot synthesis of MOF-polydopamine hybrid nanogels with enhanced photothermal effect for targeted cancer therapy, Adv. Sci. 5 (2018).
[44] S. Wei, Z. Li, W. Lu, H. Liu, J. Zhang, T. Chen, B.Z. Tang, Multicolor fluorescent polymeric hydrogels, Angew Chem. Int. Ed. Engl. 60 (2021) 8608.
[45] M.J. Ruedas-Rama, J.D. Walters, A. Orte, E.A. Hall, Fluorescent nanoparticles for intracellular sensing: a review, Anal. Chim. Acta 751 (2012) 1.
[46] B.G. Tuna, D.B. Durdabak, M.K. Ercan, S. Dogan, M. Kavruk, A.D. Dursun, S.D. Tekol, C. Celik, V.C. Ozalp, Detection of viruses by probe-gated silica nanoparticles directly from swab samples, Talanta 246 (2022), 123429.
[47] P. Srivastava, I. Tavernaro, C. Genger, P. Welker, O. Hubner, U. Resch-Genger, Multicolor polystyrene nanosensors for the monitoring of acidic, neutral, and basic pH values and cellular uptake studies, Anal. Chem. 94 (2022) 9656.
[48] X.M. Yin, L.L. Gao, P. Li, R. Bu, W.J. Sun, E.Q. Gao, Fluorescence turn-on response amplified by space confinement in metal-organic frameworks, ACS Appl. Mater. Interfaces 11 (2019), 47112.
[49] F. Luo, C. Long, Z. Wu, H. Xiong, M. Chen, X. Zhang, W. Wen, S. Wang, Functional silica nanospheres for sensitive detection of H9N2 avian influenza virus based on immunomagnetic separation, Sensor. Actuator. B Chem. 310 (2020).
[50] G. Bai, X. Xu, Q. Dai, Q. Zheng, Y. Yao, S. Liu, C. Yao, An electrochemical enzymatic nanoreactor based on dendritic mesoporous silica nanoparticles for living cell H_2O_2 detection, Analyst 144 (2019) 481.
[51] J. Li, C. Wang, W. Wang, L. Zhao, H. Han, Dual-mode immunosensor for electrochemiluminescence resonance energy transfer and electrochemical detection of rabies virus glycoprotein based on $Ru(bpy)_3^{2+}$-Loaded dendritic mesoporous silica nanoparticles, Anal. Chem. 94 (2022) 7655.
[52] M.J. Bistaffa, S.A. Camacho, W.M. Pazin, C.J.L. Constantino, O.N. Oliveira Jr., P.H.B. Aoki, Immunoassay platform with surface-enhanced resonance Raman scattering for detecting trace levels of SARS-CoV-2 spike protein, Talanta 244 (2022), 123381.
[53] J. Mei, Y. Hong, J.W. Lam, A. Qin, Y. Tang, B.Z. Tang, Aggregation-induced emission: the whole is more brilliant than the parts, Adv. Mater. 26 (2014) 5429.
[54] G. Niu, R. Zhang, X. Shi, H. Park, S. Xie, R.T.K. Kwok, J.W.Y. Lam, B.Z. Tang, AIE luminogens as fluorescent bioprobes, TrAC, Trends Anal. Chem. 123 (2020).
[55] J. Luo, Z. Xie, J.W.Y. Lam, L. Cheng, B.Z. Tang, H. Chen, C. Qiu, H.S. Kwok, X. Zhan, Y. Liu, D. Zhu, Aggregation-induced emission of 1-methyl-1,2,3,4,5-pentaphenylsilole, Chem. Commun. (2001) 1740.
[56] N. Song, Z. Zhang, P. Liu, Y.W. Yang, L. Wang, D. Wang, B.Z. Tang, Nanomaterials with supramolecular assembly based on AIE luminogens for theranostic applications, Adv. Mater. 32 (2020).
[57] W. Wu, X. Wang, M. Shen, L. Li, Y. Yin, L. Shen, W. Wang, D. Cui, J. Ni, X. Chen, W. Li, AIEgens barcodes combined with AIEgens nanobeads for high-sensitivity multiplexed detection, Theranostics 9 (2019) 7210.
[58] C. Wang, M. Liu, Z. Wang, S. Li, Y. Deng, N. He, Point-of-care diagnostics for infectious diseases: from methods to devices, Nano Today 37 (2021).
[59] L.H. Xiong, X. He, Z. Zhao, R.T.K. Kwok, Y. Xiong, P.F. Gao, F. Yang, Y. Huang, H.H. Sung, I.D. Williams, J.W.Y. Lam, J. Cheng, R. Zhang, B.Z. Tang, Ultrasensitive virion immunoassay platform with dual-modality based on a multifunctional aggregation-induced emission luminogen, ACS Nano 12 (2018) 9549.
[60] C. Yan, Y. Zhang, Z. Guo, Recent progress on molecularly near-infrared fluorescent probes for chemotherapy and phototherapy, Coord. Chem. Rev. 427 (2021).
[61] M. Zhao, B. Li, H. Zhang, F. Zhang, Activatable fluorescence sensors for in vivo bio-detection in the second near-infrared window, Chem. Sci. 12 (2021) 3448.
[62] M.E. Matlashov, D.M. Shcherbakova, J. Alvelid, M. Baloban, F. Pennacchietti, A.A. Shemetov, I. Testa, V.V. Verkhusha, A set of monomeric near-infrared fluorescent proteins for multicolor imaging across scales, Nat. Commun. 11 (2020) 239.
[63] Y. Cai, Z. Wei, C. Song, C. Tang, W. Han, X. Dong, Optical nano-agents in the second near-infrared window for biomedical applications, Chem. Soc. Rev. 48 (2019) 22.
[64] D.M. Shcherbakova, M. Baloban, A.V. Emelyanov, M. Brenowitz, P. Guo, V.V. Verkhusha, Bright monomeric near-infrared fluorescent proteins as tags and biosensors for multiscale imaging, Nat. Commun. 7 (2016), 12405.
[65] D. Kang, S. Lee, H. Shin, J. Pyun, J. Lee, An efficient NIR-to-NIR signal-based LRET system for homogeneous competitive immunoassay, Biosens. Bioelectron. 150 (2020), 111921.
[66] R.L. Pinals, F. Ledesma, D. Yang, N. Navarro, S. Jeong, J.E. Pak, L. Kuo, Y.C. Chuang, Y.W. Cheng, H.Y. Sun, M.P. Landry, Rapid SARS-CoV-2 spike protein detection by carbon nanotube-based near-infrared nanosensors, Nano Lett. 21 (2021) 2272.
[67] R. Zhang, T. Liao, X. Wang, H. Zhai, D. Yang, X. Wang, H. Wang, F. Feng, Second near-infrared fluorescent dye for lateral flow immunoassays rapid detection of influenza A/B virus, Anal. Biochem. 655 (2022), 114847.
[68] Y. Zheng, J. Wu, H. Jiang, X. Wang, Gold nanoclusters for theranostic applications, Coord. Chem. Rev. 431 (2021).
[69] Y. Xiao, Z. Wu, Q. Yao, J. Xie, Luminescent metal nanoclusters: biosensing strategies and bioimaging applications, Aggregate 2 (2021) 114.
[70] X. Kang, M. Zhu, Tailoring the photoluminescence of atomically precise nanoclusters, Chem. Soc. Rev. 48 (2019) 2422.
[71] S. Qian, Z. Wang, Z. Zuo, X. Wang, Q. Wang, X. Yuan, Engineering luminescent metal nanoclusters for sensing applications, Coord. Chem. Rev. 451 (2022).
[72] Y. Yue, T.Y. Liu, H.W. Li, Z. Liu, Y. Wu, Microwave-assisted synthesis of BSA-protected small gold nanoclusters and their fluorescence-enhanced sensing of silver(I) ions, Nanoscale 4 (2012) 2251.
[73] Y. Negishi, T. Tsukuda, Visible photoluminescence from nearly monodispersed Au12 clusters protected by meso-2,3-dimercaptosuccinic acid, Chem. Phys. Lett. 383 (2004) 161.
[74] M. Cui, Y. Zhao, Q. Song, Synthesis, optical properties and applications of ultra-small luminescent gold nanoclusters, TrAC, Trends Anal. Chem. 57 (2014) 73.
[75] M.M. Yin, W.Q. Chen, Y.J. Hu, Y. Liu, F.L. Jiang, Rapid preparation of water-soluble Ag@Au nanoclusters with bright deep-red emission, Chem. Commun. (Camb) 58 (2022) 2492.
[76] J. Xu, M. Ramasamy, T. Tang, Y. Wang, W. Zhao, K.C. Tam, Synthesis of silver nanoclusters in colloidal scaffold for biolabeling and antimicrobial applications, J. Colloid Interface Sci. 623 (2022) 883.
[77] A. Maity, A. Kumar, Higher-order assembly of BSA gold nanoclusters using supramolecular host−guest chemistry: a 40% absolute fluorescence quantum yield, Nanoscale Adv. 4 (2022) 2988.
[78] Y. Chen, M.L. Phipps, J.H. Werner, S. Chakraborty, J.S. Martinez, DNA templated metal nanoclusters: from emergent properties to unique applications, Acc. Chem. Res. 51 (2018) 2756.
[79] S. Zuo, C. Yang, J. He, Y. Liao, X. Shang, J. Gao, R. Yuan, W. Xu, Antibody-powered lighting-up fluorescence immunosensor based on hemin/G-quadruplex-quenched DNA-hosted dual silver nanoclusters as emitters, Sensor. Actuator. B Chem. 366 (2022).
[80] K. Isozaki, R. Ueno, K. Ishibashi, G. Nakano, H. Yin, K. Iseri, M. Sakamoto, H. Takaya, T. Teranishi, M. Nakamura, Gold nanocluster functionalized with peptide dendron thiolates: acceleration of the photocatalytic oxidation of an amino alcohol in a supramolecular reaction field, ACS Catal. 11 (2021), 13180.
[81] A. Nakal-Chidiac, O. Garcia, L. Garcia-Fernandez, F.M. Martin-Saavedra, S. Sanchez-Casanova, C. Escudero-Duch, J. San Roman, N. Vilaboa, M.R. Aguilar, Chitosan-stabilized silver nanoclusters with luminescent, photothermal and antibacterial properties, Carbohydr. Polym. 250 (2020), 116973.
[82] T. Zhou, Z. Su, X. Wang, M. Luo, Y. Tu, J. Yan, Fluorescence detections of hydrogen peroxide and glucose with polyethyleneimine-capped silver nanoclusters, Spectrochim. Acta Mol. Biomol. Spectrosc. 244 (2021), 118881.
[83] G. Yang, H. Zhang, Y. Wang, X. Liu, Z. Luo, J. Yao, Enhanced stability and fluorescence of mixed-proteins-protected gold/silver clusters used for mercury ions detection, Sensor. Actuator. B Chem. 251 (2017) 773.

[84] M. Wang, J. Chen, S. Jiang, Y. Nie, X. Su, Rapid synthesis of dual proteins co-functionalized gold nanoclusters for ratiometric fluorescence sensing of polynucleotide kinase activity, Sensor. Actuator. B Chem. 329 (2021).
[85] X. Chang, P. Gao, Q. Li, H. Liu, H. Hou, S. Wu, J. Chen, L. Gan, M. Zhao, D. Zhang, S. Sun, B. Wang, Fluorescent papain-encapsulated platinum nanoclusters for sensing lysozyme in biofluid and gram-positive bacterial identification, Sensor. Actuator. B Chem. 345 (2021).
[86] S. Maity, D. Bain, S. Chakraborty, S. Kolay, A. Patra, Copper nanocluster (Cu_{23} NC)-Based biomimetic system with peroxidase activity, ACS Sustain. Chem. Eng. 8 (2020), 18335.
[87] V.A. Neacsu, C. Cerretani, M.B. Liisberg, S.M. Swasey, E.G. Gwinn, S.M. Copp, T. Vosch, Unusually large fluorescence quantum yield for a near-infrared emitting DNA-stabilized silver nanocluster, Chem. Commun. (Camb) 56 (2020) 6384.
[88] Y.L. Chai, Z.B. Gao, Z. Li, L.L. He, F. Yu, S.C. Yu, J. Wang, Y.M. Tian, L.E. Liu, Y.L. Wang, Y.J. Wu, A novel fluorescent nanoprobe that based on poly(-thymine) single strand DNA-templated copper nanocluster for the detection of hydrogen peroxide, Spectrochim. Acta Mol. Biomol. Spectrosc. 239 (2020), 118546.
[89] T. Chen, S. Yang, Y. Song, J. Chai, Q. Li, X. Ma, G. Li, H. Yu, M. Zhu, All-thiolate-stabilized Ag42 nanocluster with a tetrahedral kernel and its transformation to an Ag61 nanocluster with a bi-tetrahedral kernel, Chem. Commun. 56 (2020) 7605.
[90] Y. Cao, V. Fung, Q. Yao, T. Chen, S. Zang, D.E. Jiang, J. Xie, Control of single-ligand chemistry on thiolated Au25 nanoclusters, Nat. Commun. 11 (2020) 5498.
[91] D.-Y. Qi, C. Wang, Y.-C. Gao, H.-W. Li, Y. Wu, Heteroatom doping and supramolecular assembly promoted copper nanoclusters to be a stable & high fluorescence sensor for trace amounts of ATP determination, Sensor. Actuator. B Chem. 358 (2022).
[92] Z. Huang, N. Geyer, P. Werner, J. de Boor, U. Gosele, Metal-assisted chemical etching of silicon: a review, Adv. Mater. 23 (2011) 285.
[93] T. Shu, X. Lin, Z. Zhou, D. Zhao, F. Xue, F. Zeng, J. Wang, C. Wang, L. Su, X. Zhang, Understanding stimuli-responsive oligomer shell of silver nanoclusters with aggregation-induced emission via chemical etching and their use as sensors, Sensor. Actuator. B Chem. 286 (2019) 198.
[94] J. Wang, X. Lin, L. Su, J. Yin, T. Shu, X. Zhang, Chemical etching of pH-sensitive aggregation-induced emission-active gold nanoclusters for ultra-sensitive detection of cysteine, Nanoscale 11 (2019) 294.
[95] Y. Dai, R.A. Somoza, L. Wang, J.F. Welter, Y. Li, A.I. Caplan, C.C. Liu, Exploring the trans-cleavage activity of CRISPR-cas12a (cpf1) for the development of a universal electrochemical biosensor, Angew Chem. Int. Ed. Engl. 58 (2019), 17399.
[96] P.F. Liu, K.R. Zhao, Z.J. Liu, L. Wang, S.Y. Ye, G.X. Liang, Cas12a-based electrochemiluminescence biosensor for target amplification-free DNA detection, Biosens. Bioelectron. 176 (2021), 112954.
[97] M. Shariati, Impedimetric biosensor for monitoring complementary DNA from hepatitis B virus based on gold nanocrystals, J. Electrochem. Soc. 168 (2021).
[98] Y. Chen, Y. Shen, D. Sun, H. Zhang, D. Tian, J. Zhang, J.J. Zhu, Fabrication of a dispersible graphene/gold nanoclusters hybrid and its potential application in electrogenerated chemiluminescence, Chem. Commun. (Camb) 47 (2011), 11733.
[99] Y. Wang, X. Bai, W. Wen, X. Zhang, S. Wang, Ultrasensitive electrochemical biosensor for HIV gene detection based on graphene stabilized gold nanoclusters with exonuclease amplification, ACS Appl. Mater. Interfaces 7 (2015), 18872.
[100] D. Li, B. Li, G. Lee, S.I. Yang, Facile synthesis of fluorescent silver nanoclusters as simultaneous detection and remediation for Hg^{2+}, Bull. Kor. Chem. Soc. 36 (2015) 1703.
[101] L. Shang, L. Yang, F. Stockmar, R. Popescu, V. Trouillet, M. Bruns, D. Gerthsen, G.U. Nienhaus, Microwave-assisted rapid synthesis of luminescent gold nanoclusters for sensing Hg^{2+} in living cells using fluorescence imaging, Nanoscale 4 (2012) 4155.
[102] D. Li, Z. Chen, Z. Wan, T. Yang, H. Wang, X. Mei, One-pot development of water soluble copper nanoclusters with red emission and aggregation induced fluorescence enhancement, RSC Adv. 6 (2016), 34090.
[103] C. Zheng, A.-X. Zheng, B. Liu, X.-L. Zhang, Y. He, J. Li, H.-H. Yang, G. Chen, One-pot synthesized DNA-templated Ag/Pt bimetallic nanoclusters as peroxidase mimics for colorimetric detection of thrombin, Chem. Commun. 50 (2014), 13103.
[104] P. Shah, R. Nagda, I.L. Jung, Y.J. Bhang, S.W. Jeon, C.S. Lee, C. Do, K. Nam, Y.M. Kim, S. Park, Y.H. Roh, P.W. Thulstrup, M.J. Bjerrum, T.H. Kim, S.W. Yang, Noncanonical head-to-head hairpin DNA dimerization is essential for the synthesis of orange emissive silver nanoclusters, ACS Nano 14 (2020) 8697.
[105] J. Liu, Y. Lu, L. Feng, S. Wang, S. Zhang, X. Zhu, L. Sheng, S. Zhang, X. Zhang, Pinpoint the positions of single nucleotide polymorphisms by a nanocluster dimer, Anal. Chem. 89 (2017) 2622.
[106] Y. Yuan, S. Li, L. Luo, Q. Wang, H. Fang, J. Huang, J. Liu, X. Yang, K. Wang, DNA-silver nanocluster binary probes for ratiometric fluorescent detection of HPV-related DNA, Chem. Res. Chin. Univ. 35 (2019) 581.
[107] Z. Zhou, Y. Zhang, M. Guo, K. Huang, W. Xu, Ultrasensitive magnetic DNAzyme-copper nanoclusters fluorescent biosensor with triple amplification for the visual detection of *E. coli* O157:H7, Biosens. Bioelectron. 167 (2020), 112475.
[108] H.-B. Wang, H.-D. Zhang, Y. Chen, K.-J. Huang, Y.-M. Liu, A label-free and ultrasensitive fluorescent sensor for dopamine detection based on double-stranded DNA templated copper nanoparticles, Sensor. Actuator. B Chem. 220 (2015) 146.
[109] Q. Song, Y. Shi, D. He, S. Xu, J. Ouyang, Sequence-dependent dsDNA-templated formation of fluorescent copper nanoparticles, Chemistry 21 (2015) 2417.
[110] Z. Du, L. Zhu, W. Xu, Visualization of copper nanoclusters for SARS-CoV-2 Delta variant detection based on rational primers design, Talanta 241 (2022), 123266.
[111] Y. Tao, K. Yi, H. Wang, K. Li, M. Li, Metal nanoclusters combined with CRISPR-Cas12a for hepatitis B virus DNA detection, Sensor. Actuator. B Chem. 361 (2022).
[112] W. Bian, Y. Lin, T. Wang, X. Yu, J. Qiu, M. Zhou, H. Luo, S.F. Yu, X. Xu, Direct identification of surface defects and their influence on the optical characteristics of upconversion nanoparticles, ACS Nano 12 (2018) 3623.
[113] X. Chen, J. Lan, Y. Liu, L. Li, L. Yan, Y. Xia, F. Wu, C. Li, S. Li, J. Chen, A paper-supported aptasensor based on upconversion luminescence resonance energy transfer for the accessible determination of exosomes, Biosens. Bioelectron. 102 (2018) 582.
[114] X. Jiang, X. Guo, J. Peng, D. Zhao, Y. Ma, Triplet-triplet annihilation photon upconversion in polymer thin film: sensitizer design, ACS Appl. Mater. Interfaces 8 (2016), 11441.
[115] Z. Li, H. Yuan, W. Yuan, Q. Su, F. Li, Upconversion nanoprobes for biodetections, Coord. Chem. Rev. 354 (2018) 155.
[116] F. Terenziani, C. Katan, E. Badaeva, S. Tretiak, M. Blanchard-Desce, Enhanced two-photon absorption of organic chromophores: theoretical and experimental assessments, Adv. Mater. 20 (2008) 4641.
[117] X. Zheng, R.K. Kankala, C.-G. Liu, S.-B. Wang, A.-Z. Chen, Y. Zhang, Lanthanides-doped near-infrared active upconversion nanocrystals: upconversion mechanisms and synthesis, Coord. Chem. Rev. 438 (2021).
[118] X. Ye, J.E. Collins, Y. Kang, J. Chen, D.T. Chen, A.G. Yodh, C.B. Murray, Morphologically controlled synthesis of colloidal upconversion nanophosphors and their shape-directed self-assembly, Proc. Natl. Acad. Sci. U. S. A. 107 (2010), 22430.
[119] B. Shen, S. Cheng, Y. Gu, D. Ni, Y. Gao, Q. Su, W. Feng, F. Li, Revisiting the optimized doping ratio in core/shell nanostructured upconversion particles, Nanoscale 9 (2017) 1964.
[120] B. Chen, F. Wang, $NaYbF_4$@CaF_2 core-satellite upconversion nanoparticles: one-pot synthesis and sensitive detection of glutathione, Nanoscale 10 (2018), 19898.
[121] W. You, D. Tu, R. Li, W. Zheng, X. Chen, Chameleon-like" optical behavior of lanthanide-doped fluoride nanoplates for multilevel anti-counterfeiting applications, Nano Res. 12 (2019) 1417.
[122] S. Heer, K. Kömpe, H.U. Güdel, M. Haase, Highly efficient multicolour upconversion emission in transparent colloids of lanthanide-doped $NaYF_4$ Nanocrystals, Adv. Mater. 16 (2004) 2102.
[123] G. Yi, H. Lu, S. Zhao, Y. Ge, W. Yang, D. Chen, L.-H. Guo, Synthesis, characterization, and biological application of size-controlled nanocrystalline $NaYF_4$:Yb,Er infrared-to-visible up-conversion phosphors, Nano Lett. 4 (2004) 2191.
[124] Z. Li, Y. Zhang, S. Jiang, Multicolor core/shell-structured upconversion fluorescent nanoparticles, Adv. Mater. 20 (2008) 4765.
[125] M. Liu, Z. Shi, X. Wang, Y. Zhang, X. Mo, R. Jiang, Z. Liu, L. Fan, C.G. Ma, F. Shi, Simultaneous enhancement of red upconversion luminescence and CT contrast of $NaGdF_4$:Yb,Er nanoparticles via Lu^{3+} doping, Nanoscale 10 (2018), 20279.
[126] R. Shi, X. Ling, X. Li, L. Zhang, M. Lu, X. Xie, L. Huang, W. Huang, Tuning hexagonal NaYbF4 nanocrystals down to sub-10 nm for enhanced photon upconversion, Nanoscale 9 (2017), 13739.
[127] H. Hayashi, Y. Hakuta, Hydrothermal synthesis of metal oxide nanoparticles in supercritical water, Materials 3 (2010) 3794.
[128] H. Wu, Y. Liang, Y. Ma, J. Yang, S. Hu, Up-conversion luminescence properties and temperature sensitivity of $AgBi(MoO_4)_2$: Yb^{3+}/Er^{3+}/Ho^{3+}/Tm^{3+} phosphors, CrystEngComm (2022).
[129] F. Zhang, Y. Wan, T. Yu, F. Zhang, Y. Shi, S. Xie, Y. Li, L. Xu, B. Tu, D. Zhao, Uniform nanostructured arrays of sodium rare-earth fluorides for highly efficient multicolor upconversion luminescence, Angew Chem. Int. Ed. Engl. 46 (2007) 7976.
[130] Y. Zhang, L. Huang, X. Liu, Unraveling epitaxial habits in the NaLnF4 system for color multiplexing at the single-particle level, Angew Chem. Int. Ed. Engl. 55 (2016) 5718.
[131] Q. Liu, Y. Zhang, C.S. Peng, T. Yang, L.M. Joubert, S. Chu, Single upconversion nanoparticle imaging at sub-10 W cm^{-2} irradiance, Nat. Photonics 12 (2018) 548.
[132] B. Ince, M.K. Sezginturk, Lateral flow assays for viruses diagnosis: up-to-date technology and future prospects, Trends Analyt Chem. (2022), 116725.
[133] E. Juntunen, T. Salminen, S.M. Talha, I. Martiskainen, T. Soukka, K. Pettersson, M. Waris, Lateral flow immunoassay with upconverting nanoparticle-based detection for indirect measurement of interferon response by the level of MxA, J. Med. Virol. 89 (2017) 598.
[134] M. You, M. Lin, Y. Gong, S. Wang, A. Li, L. Ji, H. Zhao, K. Ling, T. Wen, Y. Huang, D. Gao, Q. Ma, T. Wang, A. Ma, X. Li, F. Xu, Household fluorescent lateral flow strip platform for sensitive and quantitative prognosis of heart failure using dual-color upconversion nanoparticles, ACS Nano 11 (2017) 6261.

[135] Y. Gong, Y. Zheng, B. Jin, M. You, J. Wang, X. Li, M. Lin, F. Xu, F. Li, A portable and universal upconversion nanoparticle-based lateral flow assay platform for point-of-care testing, Talanta 201 (2019) 126.
[136] J. Kim, J.H. Kwon, J. Jang, H. Lee, S. Kim, Y.K. Hahn, S.K. Kim, K.H. Lee, S. Lee, H. Pyo, C.S. Song, J. Lee, Rapid and background-free detection of avian influenza virus in opaque sample using NIR-to-NIR upconversion nanoparticle-based lateral flow immunoassay platform, Biosens. Bioelectron. 112 (2018) 209.
[137] H. Zhu, F. Lu, X.C. Wu, J.J. Zhu, An upconversion fluorescent resonant energy transfer biosensor for hepatitis B virus (HBV) DNA hybridization detection, Analyst 140 (2015) 7622.
[138] M.K. Tsang, Y.T. Wong, T.H. Tsoi, W.T. Wong, J. Hao, Upconversion luminescence sandwich assay for detection of influenza H7 subtype, Adv. Healthc Mater. 8 (2019), e1900575.
[139] M.K. Tsang, W. Ye, G. Wang, J. Li, M. Yang, J. Hao, Ultrasensitive detection of Ebola virus oligonucleotide based on upconversion nanoprobe/nanoporous membrane system, ACS Nano 10 (2016) 598.
[140] Q. Zhao, P. Du, X. Wang, M. Huang, L.D. Sun, T. Wang, Z. Wang, Upconversion fluorescence resonance energy transfer aptasensors for H5N1 influenza virus detection, ACS Omega 6 (2021), 15236.
[141] Y. Zhang, L. Zhang, R. Deng, J. Tian, Y. Zong, D. Jin, X. Liu, Multicolor barcoding in a single upconversion crystal, J. Am. Chem. Soc. 136 (2014) 4893.
[142] D.H. Ortgies, M. Tan, E.C. Ximendes, B. Del Rosal, J. Hu, L. Xu, X. Wang, E. Martin Rodriguez, C. Jacinto, N. Fernandez, G. Chen, D. Jaque, Lifetime-Encoded infrared-emitting nanoparticles for in vivo multiplexed imaging, ACS Nano 12 (2018) 4362.
[143] L. Zhou, Y. Fan, R. Wang, X. Li, L. Fan, F. Zhang, High-capacity upconversion wavelength and lifetime binary encoding for multiplexed biodetection, Angew Chem. Int. Ed. Engl. 57 (2018), 12824.
[144] H. Liu, M.K. Jayakumar, K. Huang, Z. Wang, X. Zheng, H. Agren, Y. Zhang, Phase angle encoded upconversion luminescent nanocrystals for multiplexing applications, Nanoscale 9 (2017) 1676.
[145] V. Kale, H. Pakkila, J. Vainio, A. Ahomaa, N. Sirkka, A. Lyytikainen, S.M. Talha, A. Kutsaya, M. Waris, I. Julkunen, T. Soukka, Spectrally and spatially multiplexed serological array-in-well assay utilizing two-color upconversion luminescence imaging, Anal. Chem. 88 (2016) 4470.
[146] R. Wu, Z. Feng, J. Zhang, L. Jiang, J.-J. Zhu, Quantum dots for electrochemical cytosensing, TrAC, Trends Anal. Chem. 148 (2022).
[147] A.M. Wagner, J.M. Knipe, G. Orive, N.A. Peppas, Quantum dots in biomedical applications, Acta Biomater. 94 (2019) 44.
[148] R.C. Castro, D.S.M. Ribeiro, J.L.M. Santos, Visual detection using quantum dots sensing platforms, Coord. Chem. Rev. 429 (2021).
[149] M. Han, O. Karatum, S. Nizamoglu, Optoelectronic neural interfaces based on quantum dots, ACS Appl. Mater. Interfaces 14 (2022), 20468.
[150] C.B. Murray, D.J. Norris, M.G. Bawendi, Synthesis and characterization of nearly monodisperse CdE (E = sulfur, selenium, tellurium) semiconductor nanocrystallites, J. Am. Chem. Soc. 115 (1993) 8706.
[151] A.S. Novikova, C. Ponomaryova capital Te, I.Y. Goryacheva, Fluorescent AgInS/ZnS quantum dots microplate and lateral flow immunoassays for folic acid determination in juice samples, Mikrochim. Acta 187 (2020) 427.
[152] Z.A. Peng, X. Peng, formation of high-quality CdTe, CdSe, and CdS nanocrystals using CdO as precursor, J. Am. Chem. Soc. 123 (2001) 183.
[153] J.X. Soares, K.D. Wegner, D.S.M. Ribeiro, A. Melo, I. Häusler, J.L.M. Santos, U. Resch-Genger, Rationally designed synthesis of bright $AgInS_2$/ZnS quantum dots with emission control, Nano Res. 13 (2020) 2438.
[154] H. Liu, X. Lv, C. Li, Y. Qian, X. Wang, L. Hu, Y. Wang, W. Lin, H. Wang, Direct carbonization of organic solvents toward graphene quantum dots, Nanoscale 12 (2020), 10956.
[155] T. Vossmeyer, L. Katsikas, M. Giersig, I.G. Popovic, K. Diesner, A. Chemseddine, A. Eychmueller, H. Weller, CdS nanoclusters: synthesis, characterization, size dependent oscillator strength, temperature shift of the excitonic transition energy, and reversible absorbance shift, J. Phys. Chem. 98 (1994) 7665.
[156] H. Zhang, Z. Zhou, B. Yang, M. Gao, The influence of carboxyl groups on the photoluminescence of mercaptocarboxylic acid-stabilized CdTe nanoparticles, J. Phys. Chem. B 107 (2003) 8.
[157] M. Mou, Y. Wu, Q. Niu, Y. Wang, Z. Yan, S. Liao, Aggregation-induced emission properties of hydrothermally synthesized Cu-In-S quantum dots, Chem. Commun. (Camb) 53 (2017) 3357.
[158] Z. Ma, H. Ming, H. Huang, Y. Liu, Z. Kang, One-step ultrasonic synthesis of fluorescent N-doped carbon dots from glucose and their visible-light sensitive photocatalytic ability, New J. Chem. 36 (2012).
[159] M. Yao, J. Huang, Z. Deng, W. Jin, Y. Yuan, J. Nie, H. Wang, F. Du, Y. Zhang, Transforming glucose into fluorescent graphene quantum dots via microwave radiation for sensitive detection of Al^{3+} ions based on aggregation-induced enhanced emission, Analyst 145 (2020) 6981.
[160] H. Du, X. Wang, Q. Yang, W. Wu, Quantum dot: lightning invisible foodborne pathogens, Trends Food Sci. Technol. 110 (2021) 1.
[161] Z. Wang, J. Liu, G. Chen, X. Feng, M. Deng, D. Mu, Q. Xu, H. Xu, An integrated system using phenylboronic acid functionalized magnetic beads and colorimetric detection for Staphylococcus aureus, Food Control 133 (2022).
[162] X. Li, J. Li, W. Yang, D. Han, N. Yao, H. Zhao, X. Chu, X. Liang, C. Bi, C. Wang, G. Yang, Fluorescent immunosensor based on fluorescence resonance energy transfer between CdSe/ZnS quantum dots and Au nanorods for PRRSV detection, Prog. Nat. Sci.: Mater. Int. 32 (2022) 157.
[163] Y. Shao, H. Duan, L. Guo, Y. Leng, W. Lai, Y. Xiong, Quantum dot nanobead-based multiplexed immunochromatographic assay for simultaneous detection of aflatoxin B1 and zearalenone, Anal. Chim. Acta 1025 (2018) 163.
[164] J. Guo, Y. Wang, S. Niu, H. Li, Y. Tian, S. Yu, F. Yu, Y. Wu, L.E. Liu, Highly sensitive fluorescence-linked immunosorbent assay for the determination of human IgG in serum using quantum dot nanobeads and magnetic Fe3O4 nanospheres, ACS Omega 5 (2020), 23229.
[165] L. Guo, Y. Shao, H. Duan, W. Ma, Y. Leng, X. Huang, Y. Xiong, Magnetic quantum dot nanobead-based fluorescent immunochromatographic assay for the highly sensitive detection of aflatoxin B1 in dark soy sauce, Anal. Chem. 91 (2019) 4727.
[166] Z. Bai, H. Wei, X. Yang, Y. Zhu, Y. Peng, J. Yang, C. Wang, Z. Rong, S. Wang, Rapid enrichment and ultrasensitive detection of influenza A virus in human specimen using magnetic quantum dot nanobeads based test strips, Sensor. Actuator. B Chem. 325 (2020).
[167] V.T. Nguyen, S. Song, S. Park, C. Joo, Recent advances in high-sensitivity detection methods for paper-based lateral-flow assay, Biosens. Bioelectron. 152 (2020), 112015.
[168] Y. Zhou, Y. Chen, W. Liu, H. Fang, X. Li, L. Hou, Y. Liu, W. Lai, X. Huang, Y. Xiong, Development of a rapid and sensitive quantum dot nanobead-based double-antigen sandwich lateral flow immunoassay and its clinical performance for the detection of SARS-CoV-2 total antibodies, Sens. Actuators B Chem. 343 (2021), 130139.
[169] C. Wang, X. Yang, S. Zheng, X. Cheng, R. Xiao, Q. Li, W. Wang, X. Liu, S. Wang, Development of an ultrasensitive fluorescent immunochromatographic assay based on multilayer quantum dot nanobead for simultaneous detection of SARS-CoV-2 antigen and influenza A virus, Sens. Actuators B Chem. 345 (2021), 130372.
[170] J. Cheong, H. Yu, C.Y. Lee, J.U. Lee, H.J. Choi, J.H. Lee, H. Lee, J. Cheon, Fast detection of SARS-CoV-2 RNA via the integration of plasmonic thermocycling and fluorescence detection in a portable device, Nat. Biomed. Eng. 4 (2020) 1159.
[171] M. Zhang, X. Li, J. Pan, Y. Zhang, L. Zhang, C. Wang, X. Yan, X. Liu, G. Lu, Ultrasensitive detection of SARS-CoV-2 spike protein in untreated saliva using SERS-based biosensor, Biosens. Bioelectron. 190 (2021), 113421.
[172] Z. Ding, B.M. Quinn, S.K. Haram, L.E. Pell, B.A. Korgel, A.J. Bard, Electrochemistry and electrogenerated chemiluminescence from silicon nanocrystal quantum dots, Science 296 (2002) 1293.
[173] Y.P. Dong, G. Chen, Y. Zhou, J.J. Zhu, Electrochemiluminescent sensing for caspase-3 activity based on $Ru(bpy)_3^{2+}$-Doped silica nanoprobe, Anal. Chem. 88 (2016) 1922.
[174] Z. Wu, J. Hu, T. Zeng, Z.L. Zhang, J. Chen, G. Wong, X. Qiu, W. Liu, G.F. Gao, Y. Bi, D.W. Pang, Ultrasensitive Ebola virus detection based on electroluminescent nanospheres and immunomagnetic separation, Anal. Chem. 89 (2017) 2039.
[175] P.P. Dai, T. Yu, H.W. Shi, J.J. Xu, H.Y. Chen, General strategy for enhancing electrochemiluminescence of semiconductor nanocrystals by hydrogen peroxide and potassium persulfate as dual coreactants, Anal. Chem. 87 (2015), 12372.
[176] L. Liu, X. Wang, Q. Ma, Z. Lin, S. Chen, Y. Li, L. Lu, H. Qu, X. Su, Multiplex electrochemiluminescence DNA sensor for determination of hepatitis B virus and hepatitis C virus based on multicolor quantum dots and Au nanoparticles, Anal. Chim. Acta 916 (2016) 92.
[177] X.-Y. Wang, Z.-Z. Li, S.-N. Ding, A signal amplification of near-infrared electrochemiluminescence immunosensor for SFTSV determination based on SiO_2 photonic crystals nanomembrane, Sensor. Actuator. B Chem. 358 (2022).
[178] Y.Y. Zuo, W.E. Uspal, T. Wei, Airborne transmission of COVID-19: aerosol dispersion, lung deposition, and virus-receptor interactions, ACS Nano (2020).
[179] Y. Xianyu, Y. Dong, Z. Zhang, Z. Wang, W. Yu, Z. Wang, Y. Chen, Gd^{3+}-nanoparticle-enhanced multivalent biosensing that combines magnetic relaxation switching and magnetic separation, Biosens. Bioelectron. 155 (2020), 112106.
[180] R. Huang, Q. Tao, B. Chang, H. Dong, Field dependence study of commercial Gd chelates with SQUID detection, IEEE Trans. Appl. Supercond. 26 (2016) 1.
[181] Y. Li, P. Ma, Q. Tao, H.J. Krause, S. Yang, G. Ding, H. Dong, X. Xie, Magnetic graphene quantum dots facilitate closed-tube one-step detection of SARS-CoV-2 with ultra-low field NMR relaxometry, Sens. Actuators B Chem. 337 (2021), 129786.
[182] S. Tajik, Z. Dourandish, K. Zhang, H. Beitollahi, Q.V. Le, H.W. Jang, M. Shokouhimehr, Carbon and graphene quantum dots: a review on syntheses, characterization, biological and sensing applications for neurotransmitter determination, RSC Adv. 10 (2020), 15406.
[183] M.J. Molaei, Carbon quantum dots and their biomedical and therapeutic applications: a review, RSC Adv. 9 (2019) 6460.
[184] K. Hola, Y. Zhang, Y. Wang, E.P. Giannelis, R. Zboril, A.L. Rogach, Carbon dots—emerging light emitters for bioimaging, cancer therapy and optoelectronics, Nano Today 9 (2014) 590.
[185] C. He, P. Xu, X. Zhang, W. Long, The synthetic strategies, photoluminescence mechanisms and promising applications of carbon dots: current state and future perspective, Carbon 186 (2022) 91.
[186] X. Xu, R. Ray, Y. Gu, H.J. Ploehn, L. Gearheart, K. Raker, W.A. Scrivens, Electrophoretic analysis and purification of fluorescent single-walled carbon nanotube fragments, J. Am. Chem. Soc. 126 (2004), 12736.

[187] P. Zuo, X. Lu, Z. Sun, Y. Guo, H. He, A review on syntheses, properties, characterization and bioanalytical applications of fluorescent carbon dots, Microchim. Acta 183 (2015) 519.
[188] X. Wang, L. Cao, S.T. Yang, F. Lu, M.J. Meziani, L. Tian, K.W. Sun, M.A. Bloodgood, Y.P. Sun, Bandgap-like strong fluorescence in functionalized carbon nanoparticles, Angew Chem. Int. Ed. Engl. 49 (2010) 5310.
[189] J. Shen, Y. Zhu, C. Chen, X. Yang, C. Li, Facile preparation and upconversion luminescence of graphene quantum dots, Chem. Commun. (Camb) 47 (2011) 2580.
[190] Z.A. Qiao, Y. Wang, Y. Gao, H. Li, T. Dai, Y. Liu, Q. Huo, Commercially activated carbon as the source for producing multicolor photoluminescent carbon dots by chemical oxidation, Chem. Commun. (Camb) 46 (2010) 8812.
[191] J. Peng, W. Gao, B.K. Gupta, Z. Liu, R. Romero-Aburto, L. Ge, L. Song, L.B. Alemany, X. Zhan, G. Gao, S.A. Vithayathil, B.A. Kaipparettu, A.A. Marti, T. Hayashi, J.J. Zhu, P.M. Ajayan, Graphene quantum dots derived from carbon fibers, Nano Lett. 12 (2012) 844.
[192] C. Liu, G. Xiao, M. Yang, B. Zou, Z.L. Zhang, D.W. Pang, Mechanofluorochromic carbon nanodots: controllable pressure-triggered blue- and red-shifted photoluminescence, Angew Chem. Int. Ed. Engl. 57 (2018) 1893.
[193] J. Jia, Y. Sun, Y. Zhang, Q. Liu, J. Cao, G. Huang, B. Xing, C. Zhang, L. Zhang, Y. Cao, Facile and efficient fabrication of bandgap tunable carbon quantum dots derived from anthracite and their photoluminescence properties, Front. Chem. 8 (2020) 123.
[194] S.-L. Hu, K.-Y. Niu, J. Sun, J. Yang, N.-Q. Zhao, X.-W. Du, One-step synthesis of fluorescent carbon nanoparticles by laser irradiation, J. Mater. Chem. 19 (2009) 484.
[195] H. Yu, X. Li, X. Zeng, Y. Lu, Preparation of carbon dots by non-focusing pulsed laser irradiation in toluene, Chem. Commun. (Camb) 52 (2016) 819.
[196] H. Li, X. He, Z. Kang, H. Huang, Y. Liu, J. Liu, S. Lian, C.H. Tsang, X. Yang, S.T. Lee, Water-soluble fluorescent carbon quantum dots and photocatalyst design, Angew Chem. Int. Ed. Engl. 49 (2010) 4430.
[197] J. Zhou, C. Booker, R. Li, X. Zhou, T.-K. Sham, X. Sun, Z. Ding, An electrochemical avenue to blue luminescent nanocrystals from multiwalled carbon nanotubes (MWCNTs), J. Am. Chem. Soc. 129 (2007) 744.
[198] Y. Li, Y. Hu, Y. Zhao, G. Shi, L. Deng, Y. Hou, L. Qu, An electrochemical avenue to green-luminescent graphene quantum dots as potential electron-acceptors for photovoltaics, Adv. Mater. 23 (2011) 776.
[199] Y. Xu, J. Liu, J. Zhang, X. Zong, X. Jia, D. Li, E. Wang, Chip-based generation of carbon nanodots via electrochemical oxidation of screen printed carbon electrodes and the applications for efficient cell imaging and electrochemiluminescence enhancement, Nanoscale 7 (2015) 9421.
[200] Y. Li, X. Liu, J. Wang, H. Liu, S. Li, Y. Hou, W. Wan, W. Xue, N. Ma, J.Z. Zhang, Chemical nature of redox-controlled photoluminescence of graphene quantum dots by post-synthesis treatment, J. Phys. Chem. C 120 (2016), 26004.
[201] F. Niu, Y. Xu, M. Liu, J. Sun, P. Guo, J. Liu, Bottom-up electrochemical preparation of solid-state carbon nanodots directly from nitriles/ionic liquids using carbon-free electrodes and the applications in specific ferric ion detection and cell imaging, Nanoscale 8 (2016) 5470.
[202] S. Chahal, N. Yousefi, N. Tufenkji, Green synthesis of high quantum yield carbon dots from phenylalanine and citric acid: role of stoichiometry and nitrogen doping, ACS Sustain. Chem. Eng. 8 (2020) 5566.
[203] B. Zhang, C.y. Liu, Y. Liu, A novel one-step approach to synthesize fluorescent carbon nanoparticles, Eur. J. Inorg. Chem. 2010 (2010) 4411.
[204] J. Briscoe, A. Marinovic, M. Sevilla, S. Dunn, M. Titirici, Biomass-derived carbon quantum dot sensitizers for solid-state nanostructured solar cells, Angew Chem. Int. Ed. Engl. 54 (2015) 4463.
[205] S. Zhu, Q. Meng, L. Wang, J. Zhang, Y. Song, H. Jin, K. Zhang, H. Sun, H. Wang, B. Yang, Highly photoluminescent carbon dots for multicolor patterning, sensors, and bioimaging, Angew Chem. Int. Ed. Engl. 52 (2013) 3953.
[206] F. Wang, S. Pang, L. Wang, Q. Li, M. Kreiter, C.-y. Liu, One-step synthesis of highly luminescent carbon dots in noncoordinating solvents, Chem. Mater. 22 (2010) 4528.
[207] D. Pan, J. Zhang, Z. Li, C. Wu, X. Yan, M. Wu, Observation of pH-, solvent-, spin-, and excitation-dependent blue photoluminescence from carbon nanoparticles, Chem. Commun. (Camb) 46 (2010) 3681.
[208] S. Qu, X. Wang, Q. Lu, X. Liu, L. Wang, A biocompatible fluorescent ink based on water-soluble luminescent carbon nanodots, Angew Chem. Int. Ed. Engl. 51 (2012), 12215.
[209] Y. Choi, B. Kang, J. Lee, S. Kim, G.T. Kim, H. Kang, B.R. Lee, H. Kim, S.-H. Shim, G. Lee, O.-H. Kwon, B.-S. Kim, Integrative approach toward uncovering the origin of photoluminescence in dual heteroatom-doped carbon nanodots, Chem. Mater. 28 (2016) 6840.
[210] K.-R. Zhao, L. Wang, P.-F. Liu, X.-M. Hang, H.-Y. Wang, S.-Y. Ye, Z.-J. Liu, G.-X. Liang, A signal-switchable electrochemiluminescence biosensor based on the integration of spherical nucleic acid and CRISPR/Cas12a for multiplex detection of HIV/HPV DNAs, Sensor. Actuator. B Chem. 346 (2021).
[211] L. Zeng, Y. Yuan, P. Shen, K.Y. Wong, Z. Liu, Graphitic carbon-nanoparticle-based single-label nanobeacons, Chemistry 19 (2013) 8063.
[212] Y.D. Ye, L. Xia, D.D. Xu, X.J. Xing, D.W. Pang, H.W. Tang, DNA-stabilized silver nanoclusters and carbon nanoparticles oxide: a sensitive platform for label-free fluorescence turn-on detection of HIV-DNA sequences, Biosens. Bioelectron. 85 (2016) 837.
[213] R. Muszynski, B. Seger, P.V. Kamat, Decorating graphene sheets with gold nanoparticles, J. Phys. Chem. C 112 (2008) 5263.
[214] S.H. Qaddare, A. Salimi, Amplified fluorescent sensing of DNA using luminescent carbon dots and AuNPs/GO as a sensing platform: a novel coupling of FRET and DNA hybridization for homogeneous HIV-1 gene detection at femtomolar level, Biosens. Bioelectron. 89 (2017) 773.
[215] F. Xiao, W. Li, H. Xu, Advances in Magnetic Nanoparticles for the Separation of Foodborne Pathogens: Recognition, Separation Strategy, and Application, Compr Rev Food Sci Food Saf, 2022.
[216] M. Zarei-Ghobadi, S.H. Mozhgani, F. Dashtestani, A. Yadegari, F. Hakimian, M. Norouzi, H. Ghourchian, A genosensor for detection of HTLV-I based on photoluminescence quenching of fluorescent carbon dots in presence of iron magnetic nanoparticle-capped Au, Sci. Rep. 8 (2018), 15593.
[217] F. Du, Y. Chen, C. Meng, B. Lou, W. Zhang, G. Xu, Recent advances in electrochemiluminescence immunoassay based on multiple-signal strategy, Curr. Opin. Electrochem. 28 (2021).
[218] F. Rigodanza, L. Dordevic, F. Arcudi, M. Prato, Customizing the electrochemical properties of carbon nanodots by using quinones in bottom-up synthesis, Angew Chem. Int. Ed. Engl. 57 (2018) 5062.
[219] C. Pina-Coronado, A. Martinez-Sobrino, L. Gutierrez-Galvez, R. Del Cano, E. Martinez-Perinan, D. Garcia-Nieto, M. Rodriguez-Pena, M. Luna, P. Milan-Rois, M. Castellanos, M. Abreu, R. Canton, J.C. Galan, T. Pineda, F. Pariente, A. Somoza, T. Garcia-Mendiola, R. Miranda, E. Lorenzo, Methylene Blue functionalized carbon nanodots combined with different shape gold nanostructures for sensitive and selective SARS-CoV-2 sensing, Sens. Actuators B Chem. 369 (2022), 132217.
[220] J.R. Adsetts, S. Hoesterey, C. Gao, D.A. Love, Z. Ding, Electrochemiluminescence and photoluminescence of carbon quantum dots controlled by aggregation-induced emission, aggregation-caused quenching, and interfacial reactions, Langmuir 36 (2020), 14432.
[221] L. Gutierrez-Galvez, R. Del Cano, I. Menendez-Luque, D. Garcia-Nieto, M. Rodriguez-Pena, M. Luna, T. Pineda, F. Pariente, T. Garcia-Mendiola, E. Lorenzo, Electrochemiluminescent nanostructured DNA biosensor for SARS-CoV-2 detection, Talanta 240 (2022), 123203.
[222] Y.Z. Guo, J.L. Liu, Y.F. Chen, Y.Q. Chai, Z.H. Li, R. Yuan, Boron and nitrogen-codoped carbon dots as highly efficient electrochemiluminescence emitters for ultrasensitive detection of hepatitis B virus DNA, Anal. Chem. 94 (2022) 7601.
[223] J. Mehta, N. Bhardwaj, S.K. Bhardwaj, S.K. Tuteja, P. Vinayak, A.K. Paul, K.H. Kim, A. Deep, Graphene quantum dot modified screen printed immunosensor for the determination of parathion, Anal. Biochem. 523 (2017) 1.
[224] T. Guerrero-Esteban, C. Gutierrez-Sanchez, A.M. Villa-Manso, M. Revenga-Parra, F. Pariente, E. Lorenzo, Sensitive SARS-CoV-2 detection in wastewaters using a carbon nanodot-amplified electrochemiluminescence immunosensor, Talanta 247 (2022), 123543.
[225] K. Mahato, A. Srivastava, P. Chandra, Paper based diagnostics for personalized health care: emerging technologies and commercial aspects, Biosens. Bioelectron. 96 (2017) 246.
[226] L.D. Xu, F.L. Du, J. Zhu, S.N. Ding, Luminous silica colloids with carbon dot incorporation for sensitive immunochromatographic assay of Zika virus, Analyst 146 (2021) 706.
[227] L.D. Xu, J. Zhu, S.N. Ding, Immunoassay of SARS-CoV-2 nucleocapsid proteins using novel red emission-enhanced carbon dot-based silica spheres, Analyst 146 (2021) 5055.
[228] S.R. Ahmed, J. Mogus, R. Chand, E. Nagy, S. Neethirajan, Optoelectronic fowl adenovirus detection based on local electric field enhancement on graphene quantum dots and gold nanobundle hybrid, Biosens. Bioelectron. 103 (2018) 45.
[229] Y. Tian, Q. Lu, X. Guo, S. Wang, Y. Gao, L. Wang, Au nanoparticles deposited on ultrathin two-dimensional covalent organic framework nanosheets for in vitro and intracellular sensing, Nanoscale 12 (2020) 7776.
[230] H.Q. Zhao, G.H. Qiu, Z. Liang, M.M. Li, B. Sun, L. Qin, S.P. Yang, W.H. Chen, J.X. Chen, A zinc(II)-based two-dimensional MOF for sensitive and selective sensing of HIV-1 ds-DNA sequences, Anal. Chim. Acta 922 (2016) 55.
[231] J.J. Chen, T.C. Liu, Q.N. Liang, Z.N. Dong, Y.S. Wu, M. Li, Development of a time-resolved fluorescence immunoassay for Epstein-Barr virus nuclear antigen 1-immunoglobulin A in human serum, J. Med. Virol. 87 (2015) 1940.
[232] C. Chen, H. Lai, H. Liang, Y. He, G. Guo, L. Li, A new method for detection african swine fever virus: time-resolved fluorescence immunoassay, J. Fluoresc. 31 (2021) 1291.
[233] J. Wang, Q. Ma, W. Zheng, H. Liu, C. Yin, F. Wang, X. Chen, Q. Yuan, W. Tan, One-dimensional luminous nanorods featuring tunable persistent luminescence for autofluorescence-free biosensing, ACS Nano 11 (2017) 8185.
[234] L. Liang, N. Chen, Y. Jia, Q. Ma, J. Wang, Q. Yuan, W. Tan, Recent progress in engineering near-infrared persistent luminescence nanoprobes for time-resolved biosensing/bioimaging, Nano Res. 12 (2019) 1279.

Abbreviations

ACQ: aggregation-caused quenching
AIDS: acquired immune deficiency syndrome
AIE: aggregation-induced emission
AIV: avian influenza virus
ASFV: african swine fever
AuNBs: gold nanobundles

AgNCs: silver nanoclusters
AuNCs: gold nanoclusters
AuNPs: gold nanoparticles
BODIPY: boron dipyrromethene
BSA: bovine serum albumin
cDNA: complementary DNA
CDs: carbon dots
CFs: carbon fibers
COFs: covalent organic frameworks
CQDs: carbon quantum dots
CuNCs: copper nanoclusters
DMSNs: dendritic mesoporous silica nanoparticles
ECL: electrochemiluminescence
EDA: ethylenediamine
EDTA: ethylene diamine tetraacetic acid
ELISA: enzyme-linked immunosorbent assay
ENs: electroluminescent nanospheres
NCD: nanocluster dimer
NIR: near-infrared
NIRFNs: near-infrared dye-doped fluorescent nanoparticles
NMR: nuclear magnetic resonance
OA: oleic acid
ODFNs: organic dye-doped fluorescent nanoparticles
PAA: polyacrylic acid
PAMAM: polyamylamine dendrimers
PC: photonic crystal
PCR: polymerase chain reaction
PEG: polyethylene glycol
PEI: polyethyleneimine
PL: photoluminescence
PLNPs: persistent luminescence nanoparticles
PRRSV: respiratory syndrome virus
Pt NFs: platinum nanoflower
PVP: polyvinylpyrrolidone
QBs: quantum dot nanobeads
QDs: quantum dots
QDMS: quantum dot microspheres
QY: quantum yield
FAdVs: fowl adenoviruses
FLISA: fluorescent linked immunosorbent assay
FRET: fluorescence resonance energy transfer
FITC: fluorescein isothiocyanate
GQDs: graphene quantum dots
GSH: glutathione
HBV: hepatitis B virus
HIV: human immunodeficiency virus
HPV: human papilloma virus
HTLV-1: human T-lymphotropic virus type 1
IMS: immunomagnetic separation
IAV: Influenza A virus
LFA: lateral flow immunoassay
LNPs: lanthanide-doped polystyrene nanoparticles
LOD: limit of detection
LYZ: lysozyme
MB: methylene blue
MNCs: metal nanoclusters
MNPs: magnetic nanoparticles
MOFs: metal-organic frameworks
MQBs: magnetic quantum dot nanobeads
MRSw: magnetic relaxation switch
NAAO: nanoporous alumina
RABV: rabies virus
RED: rare-earth doped
RhB: rhodamine b
RI: rylenecarboximide
RSD: relative standard deviation
RT-PCR: reverse transcription-polymerase chain reaction
SARS-CoV-2: severeacute respiratory syndrome coronavirus 2
SERRS: surface enhanced resonance raman scattering
SERS: surface enhanced raman scattering
SNPs: silica nanoparticles
SPR: surface plasmon resonance
TBAP: tetrabutylammonium perchlorate
TCSPC: time-correlated single photon counting
TPA: two-photon absorption
TRFIA: Time-resolved fluorescence immunoassay
TRFNPs: time-resolved fluorescence nanoparticles
TTA: triplet-triplet annihilation
UCL: up-conversion luminescence
UCNPs: up-conversion nanoparticles
ULF: ultra-low field